

DTIC FILE COPY

4

GL-TR-89-0282

AD-A219 367

Analysis of Salmon Near-Field Data for Nonlinear Attenuation

**G. D. McCartor
W. R. Wortman**

**Mission Research Corporation
735 State Street, P.O. Drawer 719
Santa Barbara, CA 93102-0719**

October 1989

Final Report

August 1987 - October 1989

Approved for public release; distribution unlimited

**GEOPHYSICS LABORATORY
AIR FORCE SYSTEMS COMMAND
UNITED STATES AIR FORCE
HANSCOM AIR FORCE BASE, MASSACHUSETTS 01731-5000**

**DTIC
ELECTE
MAR 20 1990
S B D**

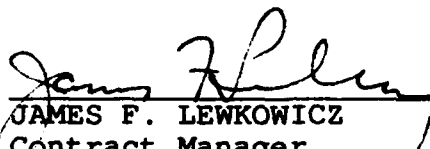
90 03 20 126

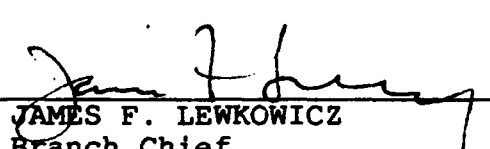
SPONSORED BY
Defense Advanced Research Projects Agency
Nuclear Monitoring Research Office
ARPA ORDER NO.5307

MONITORED BY
Geophysics Laboratory
F19628-87-C-0240

The views and conclusions contained in this document are those of the authors and should not be interpreted as representing the official policies, either expressed or implied, of the Defense Advanced Research Projects Agency or the U.S. Government.

This technical report has been reviewed and is approved for publication.


JAMES F. LEWKOWICZ
Contract Manager
Solid Earth Geophysics Branch
Earth Sciences Division


JAMES F. LEWKOWICZ
Branch Chief
Solid Earth Geophysics Branch
Earth Sciences Division

FOR THE COMMANDER


DONALD H. ECKHARDT, Director
Earth Sciences Division

This report has been reviewed by the ESD Public Affairs Office (PA) and is releasable to the National Technical Information Service (NTIS).

Qualified requestors may obtain additional copies from the Defense Technical Information Center. All others should apply to the National Technical Information Service.

If your address has changed, or if you wish to be removed from the mailing list, or if the addressee is no longer employed by your organization, please notify GL/IMA, Hanscom AFB, MA 01731-5000. This will assist us in maintaining a current mailing list.

Do not return copies of this report unless contractual obligations or notices on a specific document requires that it be returned.

UNCLASSIFIED

SECURITY CLASSIFICATION OF THIS PAGE

REPORT DOCUMENTATION PAGE

Form Approved
OMB No. 0704-0188
Exp. Date: Jun 30, 1986

1a. REPORT SECURITY CLASSIFICATION UNCLASSIFIED			1b. RESTRICTIVE MARKINGS	
2a. SECURITY CLASSIFICATION AUTHORITY			3. DISTRIBUTION/AVAILABILITY OF REPORT	
2b. DECLASSIFICATION/DOWNGRADING SCHEDULE			Approved for public release; distribution unlimited	
4. PERFORMING ORGANIZATION REPORT NUMBER(S) MRC-R-1264			5. MONITORING ORGANIZATION REPORT NUMBER(S) GL-TR-89-0282	
6a. NAME OF PERFORMING ORGANIZATION Mission Research Corporation	6b. OFFICE SYMBOL (If applicable)	7a. NAME OF MONITORING ORGANIZATION Geophysics Laboratory		
6c. ADDRESS (City, State, and ZIP code) 735 State Street, P.O. Drawer 719 Santa Barbara, California 93102-0719		7b. ADDRESS (City, State, and ZIP code) Hanscom Air Force Base Massachusetts 01731-5000		
8a. NAME OF FUNDING/SPONSORING ORGANIZATION DARPA	8b. OFFICE SYMBOL (If applicable) NMRO	9. PROCUREMENT INSTRUMENT Identification NO. F19628-87-C-0240		
8c. ADDRESS (City, State, and ZIP code) 1400 Wilson Blvd. Arlington, VA 22209-2303		10. SOURCE OF FUNDING NUMBERS		
		PROGRAM ELEMENT NO. 62714E	PROJECT NO. 7A10	TASK NO. DA WORK UNIT ACCESSION NO DE
11. TITLE (Include Security Classification) ANALYSIS OF SALMON NEAR-FIELD DATA FOR NONLINEAR ATTENUATION				
12. PERSONAL AUTHOR(S) G. D. McCartor; W. R. Wortman				
13a. TYPE OF REPORT Final	13b. TIME COVERED From 8/87 To 10/89	14. Date of Report (Year, Month, Day) 1989 October		15. PAGE COUNT 50
16. SUPPLEMENTARY NOTATION				
17. COSATI CODES			18. SUBJECT TERMS (continue on reverse if necessary and identify by block number)	
FIELD	GROUP	SUB-GROUP		
			Salmon	
			Nonlinear Attenuation	
			Partial Shear Failure	
19. ABSTRACT (Continue on reverse if necessary and identify by block number) In order to assess the existence and impact of mild nonlinear contributions to the attenuation of seismic signals from underground explosions, free-field motion data from underground 5.3 kT nuclear test Salmon have been examined. These data, which were taken at ranges from 166 to 660 meters, show moderate strains (10^{-3} to 10^{-4}) which may provide nonlinear attenuation. The attenuation over an order of magnitude in peak amplitude can be described approximately by an attenuation function Q of a bit less than 10; however, the resulting waveform is noticeably wider than the data. A linear but frequency dependent Q which decreases with decreasing frequency gives a reasonable fit to much of the waveform change as well as the peak amplitude decay with range. There remains a higher speed precursor which precedes the main pulse in the data which cannot be described by this linear Q . With a spherical finite difference calculation driven by the 166 meter				
20. DISTRIBUTION AVAILABILITY OF ABSTRACT <input type="checkbox"/> Unclassified/Unlimited <input checked="" type="checkbox"/> Same as RPT. <input type="checkbox"/> DTIC Users			21. ABSTRACT SECURITY CLASSIFICATION UNCLASSIFIED	
22a. NAME OF RESPONSIBLE INDIVIDUAL James Lewkowics			22b. TELEPHONE (Include Area Code) (617) 377-3028	22c. OFFICE SYMBOL AFGL/LWH

DD FORM 1473, 84 MAR

83 Apr edition may be used until exhausted.

SECURITY CLASSIFICATION THIS PAGE

All other editions are obsolete

UNCLASSIFIED

UNCLASSIFIED

SECURITY CLASSIFICATION OF THIS PAGE

19. ABSTRACT (Continued)

Salmon pulse, it is found that a rapid shear modulus decrease at a 10^{-4} strain threshold can reproduce the observed precursor and other features of the pulses at greater ranges when a linear absorption band $Q \approx 10$ is also added. The attenuation of the Salmon pulse is thus partly attributable to a nonlinear effect of material failure as well as a conventional linear mechanism.

Accession For	
NTIS GRA&I	<input checked="checked" type="checkbox"/>
DTIC TAB	<input type="checkbox"/>
Unannounced	<input type="checkbox"/>
Justification	
By	
Distribution/	
Availability Codes	
Dist	Avail and/or Special
A-1	



SECURITY CLASSIFICATION THIS PAGE

UNCLASSIFIED

This final technical report consists of a list and summary of the reports written under this contract together with a preprint of a paper which will be submitted for open publication.

Scientific Report #1: SEISMIC MONITORING OF A THRESHOLD TEST BAND TREATY (TTBT) FOLLOWING CALIBRATION OF THE TEST SITE WITH CORRTEX EXPERIMENTS by R. W. Alewine, III, H. D. Grey, G. D. McCartor and G. L. Wilson, Report AFGL-TR-88-0055.

The problem of monitoring a TTBT using seismic data following calibration of the test site with CORRTEX experiments is studied. Results are presented for the case of one or two CORRTEX experiments and also for the more general case of several such experiments. A number of possible monitoring procedures are studied and compared. The difference in the procedure is the amount of information available, prior to the CORRTEX experiments, on the quantity σ_{SEI} , the standard deviation of measurements of the log of the yield as measured by seismic techniques. Procedures studied involve assumptions of knowledge of σ_{SEI} which include the assumption that σ_{SEI} is known; a bound on σ_{SEI} is known; an estimate of σ_{SEI} sufficiently accurate for specified uses is known; and σ_{SEI} is unknown.

Scientific Report #2: FURTHER STATISTICAL STUDIES OF THE YIELDS (U) by G. D. McCartor, R. Blandford and R. W. Alewine, III, Report AFGL-TR-88-014(S).

In this report we present further work on the procedure of combining m_b , L_g and M_o measurements of underground tests at the Shagan River test site and of the implications of the combined estimates of the yields for monitoring treaties regarding tests at that site. We argue that the analysis presented in previous work, supplemented by some further analysis presented in the present document, provides strong support for the following conclusions: (1) The Shagan River test site should be broken into geographically distinct regions with a relative bias between the regions used for yield

estimation; (2) The relative bias between the regions labeled North and West is approximately 0.11 log-yield units; the relative bias between the regions labeled West and Central is approximately 0.075 log-yield units; and (3) When the unified seismic method is used and the suggested geographical corrections are made, the resulting precision of the measurements for yields near that of the largest source in the data is quite high, corresponding to an F-number of about 1.21 or less, while the high precision may obtain at smaller yields there is not good evidence for this conclusion in the current data and the precision at smaller yields may degrade to an F-number of about 1.3.

Scientific Report #3: NONLINEAR ATTENUATION MECHANISM IN SALT AT MODERATE STRAIN BASED ON SALMON DATA by G. D. McCartor and W. R. Wortman, Report AFGL-TR-89-0013.

In order to describe the seismic pulse or source function from UGTs outside the region of nonlinear attenuation, data from the Salmon even (5.3 kT in salt) have been examined to serve as the basis for a description of a mild nonlinear attenuation mechanism. It is found that a precursor in the Salmon pulses can be attributed to a partial shear failure of the medium which operates above a compressional strain threshold of about 10^{-4} . When this loss mechanism is included along with a linear Q of about 10, the Salmon pulses in the moderate strain regime are nearly reproduced in both amplitude and shape. Using this result the pulse can be propagated out to a range for which no further shear failure occurs and it can serve as a linear source function.

The article entitled ANALYSIS OF SALMON NEAR-FIELD DATA FOR NONLINEAR ATTENUATION by G. D. McCartor and W. R. Wortman follows.

ANALYSIS OF SALMON NEAR-FIELD DATA FOR NONLINEAR ATTENUATION

G. D. McCartor and W. R. Wortman
Mission Research Corporation
Santa Barbara, California

Abstract

In order to assess the existence and impact of mild nonlinear contributions to the attenuation of seismic signals from underground explosions, free-field motion data from underground 5.3 kT nuclear test Salmon have been examined. These data, which were taken at ranges from 166 to 660 meters, show moderate strains (10^{-3} to 10^{-4}) which may provide nonlinear attenuation. The attenuation over an order of magnitude in peak amplitude can be described approximately by an attenuation function Q of a bit less than 10; however, the resulting waveform is noticeably wider than the data. A linear but frequency dependent Q which decreases with decreasing frequency gives a reasonable fit to much of the waveform change as well as the peak amplitude decay with range. The higher speed precursor which precedes the main pulse in the data cannot be described by this linear Q . With a spherical finite difference calculation driven by the 166 meter Salmon pulse, it is found that a rapid shear modulus decrease at a 10^{-4} strain threshold can reproduce the observed precursor and other features of the pulses at greater ranges when a linear absorption band $Q \approx 10$ is also added. The attenuation of the Salmon pulse is thus partly attributable to a nonlinear effect of material failure as well as a conventional linear mechanism.

INTRODUCTION

Near-field pulses from underground explosions certainly exhibit nonlinear behavior, at least out to a radius for which gross structural changes in the rock appears. Beyond this radius (roughly 100 meters/kiloton^{1/3}) for strains less than 10^{-3} , but before linear level strains of 10^{-6} are reached, there may be subtler nonlinear

changes that influence propagation. For the purposes of establishing a seismic source function [Mueller and Murphy, 1971. Von Seggern and Blandford, 1972, Masse, 1981], it is common to determine a range beyond which the pulse is taken as linear, as indicated by experimental data indicating a nearly constant reduced displacement potential. Typically this "elastic radius" is taken at a few hundred meters/ $kt^{1/3}$. In relating teleseismic observations and implied source characteristics it is assumed that the signal propagates linearly with some attenuation imposed in the form of a Q function. However, if there is significant contribution from nonlinear behavior, the resulting teleseismic waveforms may be in error. Here we examine the Salmon near-field data where the strains are in transition from highly nonlinear crushing to a linear regime that can be described by Q in order to identify any clear evidence of nonlinear behavior and to provide a description of the mechanism that produces it.

PREVIOUS WORK

Of the large body of information available for the propagation of seismic signals in the intermediate strain regime, corresponding to strains varying from about 10^{-3} to about 10^{-6} , the data for salt appear to be the most nearly complete [McCartor and Wortman, 1985]. Data from the Salmon nuclear explosion [Perret, 1967 and Rogers, 1966], the Cowboy series of chemical explosions [Murphey, 1961 and Minster and Day, 1986] and Larson's [1982] data on laboratory chemical explosions provide propagation data in the relevant strain regime for a wide range of yields (approximately ten orders of magnitude), distances and characteristic frequencies [Trulio, 1976]; the range of scaled distances (distance/yield $^{1/3}$) is a factor of about 300 while the range of characteristic frequencies is nearly four orders of magnitude. The propagation of pulses from explosions approximately satisfies cube-root scaling: if distances and times are scaled by the cube root of the yield, the waveforms and amplitudes from all events are nearly the same even though at least some portion of the data is presumably in the nonlinear regime. Furthermore, the propagation provides a waveform which changes only slowly with distance.

Salt is a relatively uniform medium for which there are a variety of experiments ranging from Salmon, through the Cowboy series to small laboratory explosions as reported by Larson. The experiments of Larson for small chemical explosions in pressed salt have provided pulses over a scaled range from $10 \text{ m/kt}^{1/3}$ to $200 \text{ m/kt}^{1/3}$. The dominant range of frequencies covered was from about 10^4 to 10^5 Hz and the ratio of peak particle velocities to compressional sound speed (which is comparable with the strain) went from about 10^{-1} to less than 10^{-3} ; by most standards this would suggest that the response was nonlinear. Yet, by performing a direct superposition experiment with a pair of simultaneous explosions, it was found that the resulting response was consistent with direct addition of the two pulses as would be expected from a linear medium. Still it is not clear just how nonlinear effects would be manifest in this experiment without knowing the character of any nonlinear behavior. That is, the apparent success of superposition for pulses with large strains may not directly negate the possibility of any sort of nonlinear behavior [S. M. Day, private communication, 1989]. The Cowboy series of chemical explosions had a range of yields from 10 to 2000 pounds of TNT, some of which were carried out in cavities for decoupling tests. The scaled ranges for the coupled experiments were from 200 to 3000 $\text{m/kt}^{1/3}$ and the corresponding peak strains were from a few times 10^{-4} to about 10^{-5} . The dominant frequencies were 10 to 10^2 Hertz. The Salmon event took place in a natural salt dome; a comprehensive set of measurements were taken, both at surface and subsurface locations. Subsurface measurements included scaled ranges from 100 $\text{m/kt}^{1/3}$ to about 425 $\text{m/kt}^{1/3}$, which provided peak strains from about 4×10^{-3} to about 3×10^{-4} with dominant frequencies from 1 to over 10 Hertz. The Salmon data show remarkable internal consistency and correspond well with the other salt data.

Peak velocity data from the salt shots are shown as a function of scaled range in Figure 1. The scaled data from a huge range of yields tend to fall nearly on a straight line indicating a power law behavior with an exponent of about -1.9. This contrasts with a value of -1 which would be expected for pure elastic behavior. Simple scaling with yield appears to hold over this great range of strains. Note again that the range of yields over which simple scaling holds includes strains which are expected

to give nonlinear behavior. However, deviation from r^{-1} behavior is not necessarily a nonlinear effect. In particular, linear but inelastic (i.e., anelastic) behavior can provide such results.

Trulio [1976] has noted that the Salmon data for decay of peak velocity with range are consistent with an effective Q of about 5. The effective Q for this process tends to increase with increasing frequency and increase with decreasing strain. Note that simple scaling, in conjunction with linearity, indicates that Q must be independent of frequency as well as amplitude. To some degree, dependence on both variables is subject to experimental examination. Gupta and McLaughlin [1989] have analyzed some Salmon and Sterling data and concluded that the effective Q at Salmon strains appears to be strain and frequency-dependent. Q is 5 to 10 and appears to increase mildly with increasing range. Q is also larger at higher frequencies above the corner. Sterling data, which are at lower strains, are less cohesive but they suggest a significantly larger Q consistent with a transition to a linear low attenuation at small strains. Langston [1983] indicates that Sterling S-waves, generated by asymmetries in the existing Salmon cavity, show a Q_β of about 35 suggesting a P-wave Q of about 70. Denny [1989] says that the source spectra characteristics of Salmon and Sterling indicate that the Salmon pulses are nonlinear to beyond 700 meters.

Minster and Day [1986] have used the scaled peak velocity data for Cowboy to determine if these data require an amplitude (nonlinear) or frequency-dependent Q for consistency. It is determined that a Q^{-1} which consists of a small constant plus a term proportional to the peak strain provides a good fit to the data when applied in a piecewise linear fashion. The observed attenuation effects do not firmly indicate the need for a frequency-dependent Q , but indicate that an amplitude dependent Q provides a much more convincing fit than a constant Q . It is concluded that there must be nonlinear attenuation in the Cowboy strain regime.

The work of Larson [1982] on laboratory explosions in pressed salt indicates that superposition appears to hold at a strain level of about 10^{-3} . However, data from three sensors at increasing ranges provide increasing values of Q from 12 to 25 with

increasing range for ranges of 30 to 70 m/kt^{1/3}. A constant Q cannot describe the results.

New England Research laboratory ultrasonic pulse propagation experiments [Coyner, 1988] have strains from less than 10⁻⁶ to more than 10⁻⁵. In these experiments compressional and shear ultrasonic pulses consisting of about two cycles at 100-200 kHz were propagated through samples. Attenuations were calculated using a spectral ratio technique. Variation of the attenuation with peak strain amplitude and confining pressure were determined. For dome salt it was found that over a strain range of 5x10⁻⁷ to 3x10⁻⁵ and for a confining load range of 0.1 to 1 MPa, the P-wave attenuation is nearly constant and can be described by a Q of about 20. There is no particular evidence of nonlinearity in these data alone although the attenuation is large. It should be noted that these confining pressures are small compared with those for underground sources.

There exist laboratory data on the absorption of the energy in small oscillations of halite rods taken by Tittmann [1985]. These experiments on decay of cyclic motion induced in salt samples indicate that for strains below 10⁻⁶, and confining pressures consistent with that for underground explosions, a value of Q of several hundred is appropriate. For larger strains the value of Q decreases indicating a nonlinear attenuation although the nonuniform nature of the deformations in the experiment makes it difficult to extract Q as a function of strain.

These salt data generally indicate that for strains in excess of 10⁻⁵ there is an attenuation which is probably nonlinear, increases with increasing strain and can be described by an effective Q of the order of 10 for the dominant frequencies in the pulses. No detailed knowledge of the attenuation mechanism currently exists but there does appear to be a consistency in that the explosively generated pulses closely obey simple scaling. This suggests that the mechanism must be rate independent. Data for strains near 10⁻⁶ are not so consistent but they come from limited and diverse experiments. Generally, attenuation decreases to a modest level for strains less than 10⁻⁶ and then is presumably linear.

SALMON DATA AND NONLINEAR BEHAVIOR

We shall now consider the extent to which Salmon data can shed light on the issue of linear versus nonlinear behavior beyond the "elastic radius" by exploring the consequences of the assumption of linear behavior. This will be done by examination of a series of velocity records from subsurface sensors to see if they are consistent with strictly linear behavior. We shall attempt to determine if the records exhibit features that cannot be understood in terms of linear attenuation which is possibly a function of frequency. If the data are consistent with attenuation which is independent of amplitude, but is possibly a function of frequency, they may allow the possibility that the propagation mechanism is linear without ruling out a nonlinear effect. However, even then it can serve to rule out a wide range of possible nonlinear mechanisms.

SALMON DATA

Data records for Salmon were taken by either velocity and acceleration gauges, oriented either horizontally or vertically [Perret, 1967]. The horizontal gauges were either aligned radially from the source or transverse to this direction (to check for asymmetries). The raw acceleration data allow determination of velocity by integration. Two problems arise. First, the resulting velocity generally not only does not go to a constant, but it increases at a constant rate; this is a result of a post-shot non-zero baseline for the acceleration instruments. It must be corrected for by altering the acceleration baseline at late-times. There is a problem beyond this because even when the late-time acceleration is taken as zero, the late-time velocity, while now forced to be constant, is generally not zero. This may be a result of clipping of the acceleration peak due to inadequate instrument response or to inadequate bandwidth in recording. It is impossible to correct the difficulties in a unique manner. However, it appears to be possible to do so in such a way that the effect on conclusions drawn from the result will not be important. We have chosen to correct the data as follows: first, the raw velocity records (or once integrated acceleration records) were fit at late time with a straight line from a late time (1.6 sec) back to the time of the initial positive peak in such a way as to give a behavior past the peak which was consistent with the results

shown by Perret, who had access to complete instrument performance data as well as substantial insight into experimental details; the resulting linear trend was then removed; the velocity points before the peak were then altered by multiplication of each data value by the ratio of the new peak value to the old peak value. This assures that the velocity will be continuous and that the leading edge retains its original character although with a mild discontinuity in the first derivative exactly at the peak. It is impossible to detect this discontinuity by merely looking at the resulting plotted velocities. The effects of this correction will be seen primarily in the high frequency end of the spectra and this will not be the region of interest. In addition to altering the raw data records for obvious instrumentation problems, we have at the same time introduced a geometrical factor which provides an estimate of the spherical radial velocity from each record. Since all six of the records chosen for use are of horizontal radial motion, the corresponding spherical motion can be estimated by assuming the observed results are just the component of spherical radial motion.

The six records selected for study include those at ranges from 166 to 660 meters. The records were selected so as to have as large a set of ranges as possible while also having them be as internally consistent as possible. Consistency was established by taking records whose peak velocities fell along a smooth curve when plotted against range. While there is no real reason to believe that any one of the records is more desirable than some which were rejected, our use of spectral ratio methods requires avoiding examples which will obviously lead to unreasonable results when records are used in pairs. The records selected are indicated in Table 1 along with some of their properties.

The available data records extend out to about five seconds past the explosion and consist of values every 0.2 milliseconds. It was found that after about 1.5 seconds the records showed no further significant contribution, so we truncated the data at 1.6 seconds giving a convenient 8192 data points for each record. The corrected velocity records, all but one of which were taken from acceleration data, are shown on Figure 2. When plotted on the same scale it becomes difficult to appreciate

fully the features of the more distant examples, so the same data are plotted again in Figure 3, normalized to unit peak amplitude.

PRECURSOR

The Salmon data have a feature which may be useful in understanding some nonlinear effects of attenuation. Each of the pulses experimentally observed at six sensors at ranges from 166 meters to 660 meters exhibits a discontinuity in the slope upon the initial steep rise in pulse velocity, as seen in Figure 3. This appears as a toe-like behavior in the leading edge of the velocity profile which has been described by Perret as an "elastic precursor" to the main pulse. The absolute amplitude of the toe remains approximately constant with range, at a particle velocity of about 0.5 m/s, while its amplitude relative to the peak increases with range. This precursor amplitude corresponds to a compressional strain level of $\epsilon \approx 10^{-4}$. The leading edge of the pulses (i.e., that disturbance earliest in time) propagates at a speed of about 4.7 km/sec while the pulse peaks, always after the toe, propagate at a speed of about 3.7 km/sec. The elastic compressional speed of mild disturbances in this salt medium found from independent measurements were typically about 4.6 km/sec. This indicates that the precursor signal seen in the Salmon data is due to elastic behavior while the subsequent pulse suffers a lower propagation speed due to some relaxation or plastic behavior.

Perret suggests that an elastic-plastic material behavior might account for the data in perhaps one of two ways. First, the precursor could develop at large strain, where an elastic limit is exceeded from radii much smaller than instrumented for Salmon, and continue to propagate in front of a following plastic wave. Second, it may be that the precursor develops in the moderate strain region if dome salt has an elasto-plastic nature at such strains. In either case, the modulus of salt must be a function of the strain - that is, the medium is nonlinear.

If the precursor develops at large strain there must be an elastic limit beyond which plastic behavior provides a lower modulus. When such a medium is dynamically

loaded beyond the elastic limit, a leading pulse at the elastic limiting stress is generated followed by a larger amplitude but slower plastic wave. If the elastic-plastic transition is not sharply defined, the resulting pulse could consist of a gently rising leading elastic front which smoothly merges with the main plastic pulse much as seen in the Salmon data. Perret points out that if some energy from the plastic component is fed to the elastic portion during propagation, the amplitude of the elastic piece could remain nearly constant, but this is quite speculative. What is known is that a variety of laboratory experiments show that strong impulsive sources can produce elastic precursors in a variety of media. For example, work of Ahrens and Duvall [1966] with planar pulses in quartz generated by explosives exhibit an apparent elastic stress limit of about 70 kbar corresponding to strains of about 10^{-1} . This produces a leading edge, described as the elastic shock, which propagates at a speed in excess of that of the deformational portion of the pulse which follows. The elastic shock propagates with an equivalent modulus which is greater than the static modulus at this high stress. It is speculated that the elastic wave is supported by a higher than equilibrium shear stress. After the elastic component has passed, the shear stress is apparently reduced to the static value by a plastic or fracture process. This experiment, as well as that by Taylor and Rice [1963] which also shows an elastic precursor, provides elastic limits of many or tens of kilobars in contrast with the Salmon data since they give a precursor amplitude of about 5 bars. Consequently this mechanism does not seem a likely means of accounting for the Salmon data since they give a nearly constant and small precursor amplitude which seems to begin near the 166 meter sensor range rather than be well developed by this time.

The second possibility indicated by Perret is that of having the precursor develop locally in the observation region based on moderate strain plastic behavior. While there is no accepted dynamical equation of state for dome salt, Perret points out that dome salt is known to be highly plastic: under static conditions, it is nearly hydrostatic. Thus plastic deformation of salt at moderate stresses is apparently normal. In order to account for the precursor data in Salmon, the equation of state would have to provide linear behavior up to a threshold (a threshold of about 5 bars, much

less than the 70 kbars found for the elastic shock discussed above) and, through some deformation of the material, relax the modulus abruptly (on the Salmon time scale) to a value which provides a compressional propagation speed about 20% less than for infinitesimal strains in undisturbed material.

DATA ANALYSIS

The amplitudes of Figure 2 indicate that the pulse progresses smoothly to large radii (with a decrease in amplitude which is approximately like radius to the -1.9 power). At the same time, Figure 3 indicates that the normalized pulse shape remains fairly stable but it shows a mild tendency to smooth out the sharp peak and to increase the width. These features suggest that the higher frequency components are being more rapidly attenuated than the low as would be appropriate, for example, with a constant Q , should such a description be suitable. Beyond this, there is the initial ramp or precursor on each pulse which strengthens relative to the peak amplitude as the radius increases. In order to establish the possible nonlinear character of the Salmon data, we shall adopt the position of exploring the consequences of the assumption of anelastic behavior as expressed in terms of a Q function which we will attempt to evaluate. If this attempted description leads to contradictions, such as an effective Q that depends upon amplitude, we shall attribute the effects to nonlinear behavior. We shall use the data to make estimates of Q over a range of frequencies and amplitudes. Since we are dealing with data exclusively from a single event, no assumptions about the scaling behavior are necessary and no such information will be gained.

A strict interpretation of anelastic behavior would require that we find a Q function, dependent generally upon frequency, as well as a phase velocity c which is consistent with Q , so as to enforce the requirement of causality [Aki and Richards, 1980]. However, moderate values of Q are consistent with a nearly constant c , at least over the range of frequencies which are available to experimental verification. As indicated by Kjartansson [1980] and generalized to spherical geometry by McCarter and Wortman [1985], the propagation of a pulse in an anelastic medium with Q independent of frequency can be given analytically. This leads to frequency domain

representation of the change of the Fourier transform of the velocity in going from radius 'a' to 'r' as

$$\exp\left(\frac{-\omega(r-a)}{2cQ}\right) = \left| \frac{\tilde{v}(r, \omega)}{\tilde{v}(a, \omega)} \right| \left| \frac{\frac{i\omega}{ca} - \frac{\omega}{2cQa} - \frac{1}{a^2}}{\frac{i\omega}{cr} - \frac{\omega}{2cQr} - \frac{1}{r^2}} \right| \quad (1)$$

where c is a mild function of frequency and Q given by Kjartansson. This relation allows the testing of changes in velocity pulses to determine if they are consistent with this constant Q . It can also be viewed as a means of estimating this Q from velocity data pairs. If the $1/Q$ terms on the right hand side is dropped, as is suitable for Q much larger than one, we arrive at the common operational definition of Q which can be used to solve directly for it, given c . Here c will be taken as a constant at 3.7 km/sec, the speed of the main peak.

Estimates of Q have been carried out for all adjacent pairs of records along with the extreme pair. In each case, the velocity spectra ratio has been corrected for instrument response [Perret, 1967] using the frequency domain response function of the sensors. These corrections are generally fairly small. Figure 4 shows the estimates of Q obtained using Equation 1 with the Salmon velocity data records for the closest pair at ranges of 166 and 225 meters; Figure 5 shows the corresponding Q for the farthest pair at 402 and 660 meters; finally, Figure 6 gives Q for the extreme pair at 166 and 660 meters. The resulting effective Q s are remarkably similar for all pairs. There appears to be no significant difference between the initial and final record pair estimate for Q , especially at frequencies near the corner. (There does appear to be a mild tendency for a larger attenuation at smaller ranges but given the scatter of the data this cannot be firmly interpreted as evidence of nonlinearity. Gupta and McLaughlin, using a different data set and a different analysis, suggest that the effective Q does change significantly over this range although a flat Q is within the limits of their uncertainty.) However, the results consistently indicate a dependence on frequency. To determine better if a constant Q fit is adequate, the initial pulse at 166 meters has been propagated using Kjartansson's model for $Q = 10$ with $c =$

3.7 km/s at 1 Hz. This value of Q gives a good fit to the changes in the peak pulse amplitude. The scaled pulse shapes that result from this assumption are given in Figure 7 and they can be compared directly with the data in Figure 3. Generally the constant Q calculation gives pulses which are broader and less peaked than the data. If a model for a frequency dependent Q is taken as

$$Q^{-1} = 1/20 + 1.5/f \quad (2)$$

from an approximate fit to the data (this Q is linear in f until roughly 30Hz, when it becomes constant), along with constant c , the propagation of the initial 166 meter data by Fourier synthesis again gives a good fit to the peak amplitude decay. The resulting pulse shapes, scaled to unit amplitude, are given in Figure 8. This approximation to Q provides a better fit to the peak width and sharpness. Note that the precursor seen on each of the original data records cannot be obtained by this simple linear model.

PRECURSOR ANALYSIS

The technique which we have used is that of taking the observed Salmon initial velocity pulse at small range (166 meters) as a source and comparing the resulting pulses as they are propagated through material subject to candidate constitutive relations. The results are compared with observed signals at larger ranges. For any constitutive relation the effective Q associated with the attenuation may be determined, but it must be emphasized that nonlinear attenuation cannot be properly described by a Q function. The fundamental comparison of the data with calculations is not in terms of the Q but in terms of reproduction of waveform including both amplitude and shape.

As an equation of state hypothesis which can be consistent with the Salmon data, consider a medium for which the shear modulus permanently (or at least, does not recover until the pulse is past) decreases upon having a critical strain threshold exceeded; the compressional modulus before and after exceeding the strain threshold reflects the compressional speeds at the beginning and peak of the Salmon pulses,

respectively. This will be referred to as a shear failure model. Depending upon the relation between the compressional and the shear moduli, complete shear failure may occur, meaning that the elastic shear modulus, μ , goes to zero. For the example used in this discussion, the compressional speed decreases to 80% of its original value. We have taken the Lamé constants λ and μ to have a ratio of 2. Thus a decrease of the compressional speed, $((\lambda + 2\mu)/\rho)^{1/2}$, where ρ is the density, of 20% corresponds to reducing μ to about 38% of its elastic value when λ is held fixed. Note that the reduction of modulus at a fixed strain is consistent with scaling since the strain is a unitless quantity and there is no rate dependence. The scaling restriction does require that the relaxation time of the modulus change be short compared with any representative time scale of the data; we take the transition to be instantaneous. In order to determine the effect on the pulse propagation we use the observed Salmon velocity at 166 meters as the source. These calculations were carried out using a standard finite difference method as illustrated by Wilkins[1964].

As an initial effort, the elastic threshold was taken at a compressional strain of 10^{-4} ; the resulting pulse sequence at the ranges to observation stations for Salmon is as shown in Figure 9. Note that the character of the calculated precursor is much like that seen experimentally, in Figure 2, in that the leading feature is drawn out, the transition to the main pulse takes place at a constant amplitude and the peak now moves at a significantly lower speed. Still the amplitude of the main peak does not decrease as quickly as the data indicate.

When the modulus decreases, the elastic energy in the pulse also decreases in a manner approximately proportional to the square of the compressional wave speed. Since the modulus reduction is permanent, this energy is lost to the pulse and goes into heating the medium. For the parameter used, over a full cycle for which most of the pulse exceeds the critical strain, approximately one-third of the original elastic energy will be lost. This corresponds to an effective Q of about 13 for peak strains well in excess of 10^{-4} (for small strains less than this threshold, there will be no loss). This value of Q is far less than that expected for very small strains but it is still more than the 5 to 10 seen for Salmon attenuation. The addition of a

moderate level of linear attenuation consistent with that seen for small to moderate strains in other experiments will improve the agreement (for example, the NER data suggest $Q \approx 20$). More importantly, the use of a partial shear failure mechanism will automatically terminate once the pulse weakens so that the peak strain falls below the critical strain threshold value. This will produce a sharply changing effective Q in a manner suggested by the Cowboy data.

The attenuation from partial shear failure alone does not produce an amplitude for the pulse at 660 meters which is as small as that seen experimentally. More attenuation can be added to attempt to match better the data by employing a linear Q of sufficient value. A method of inclusion of a linear absorption band Q in time stepping finite difference methods has been demonstrated by Day and Minster [1984] through use of Padé approximants. Our application of this method is outlined in the Appendix. This formalism was employed using a target Q of 10 with a range of half amplitude frequencies of 1 to 100 Hertz (Q rises above 20 beyond these values). The sequence of pulses that results using both the partial shear failure and a linear Q of 10, starting with the Salmon pulse at 166 meters, is shown in Figure 10. The amplitudes for the main peaks now are in substantial agreement with the data and the length and amplitude of the precursor are also reproduced fairly well. There remains a very abrupt transition from precursor to main pulse which is clearly sharper than the experimental data. In order to avoid the abrupt transition between precursor and pulse a range of the threshold for the shear failure has been added to the model. This allows a variation of failure threshold values of compressional strain over a range of $\pm 30\%$ with a constant probability about the 10^{-4} value. Each cell in the finite difference calculation is given its own threshold which is randomly chosen on this basis. The set of pulses at the Salmon instrument ranges then calculated is given in Figure 11. The result is a smoother transition from precursor to main pulse in a manner which is quite similar to the actual Salmon data shown in Figure 2. While it is possible to achieve a detailed fit to the data by further such refinements, this is not a very meaningful thing to do since the mechanisms are not understood to the required level of detail. The important point is that it is possible to reproduce the

data to a substantial degree using only a few physically based parameters to describe the thresholded partial shear failure. Rimer and Cherry [1982] have shown that it is possible to reproduce the Salmon data, including the precursor, using a shear strength limit which is variable. The yield strength is initially weak but then strengthens and weakens again through quadratic work hardening. This phenomenological constitutive relation will not provide scaling.

DISCUSSION

Free field ground motion data from Salmon at ranges of 166 to 660 meters have been examined in order to determine if the associated attenuation of amplitude and distortion of pulse shape imply operative nonlinear effects in this moderate strain regime. This has been done by attempting to account for the data using only a linear description such that a failure would clearly indicate the alternative, nonlinear behavior. It is found that within the limits of accuracy of the experimental data, and ignoring the precursor, it is possible to account for these Salmon data using a strictly linear attenuation model with a frequency dependent Q which is the order of ten. These limited data are consistent with linear behavior, but they do not explicitly rule out nonlinear mechanisms. It seems certain that the attenuation at lesser strains must decrease to meet the rather larger Q indicated by data from other experiments at strains approaching 10^{-6} .

The elastic precursor or leading toe seen in Salmon near-field, moderate strain, velocity data is reproduced rather well with the hypothesis of partial shear failure which is activated for the duration of the pulse when the compressional strain exceeds 10^{-4} . This also gives an attenuation mechanism which accounts for much of the energy loss seen in the decay of pulses from Salmon with range. However, the overall attenuation produced is not quite adequate to account for that seen in the data. The addition of a linear absorption band attenuation, which is active over much of the significant frequency range appropriate to Salmon and which has a Q of 10, then provides a propagation model which nearly reproduces the signals at ranges beyond 166 meters when the observed signal at this range is used as the source. Furthermore,

this threshold mechanism provides a transition to more modest attenuation at small strains which is required to be consistent with Cowboy data; when applied to different yield events in salt, it will produce simple scaling as observed over a wide range of explosive events. While there is no assurance that this mechanism applies in other than the salt medium, Perret points out that elastic precursors of a similar character have been seen in underground test pulses in both alluvium and dolomite. The fact that the reduction in compressional wave speed is attributed to shear failure, rather than alteration of some other material property, is largely a matter of consistency with past thinking on modes of material behavior; there is no direct experimental link to shear properties. The general agreement with data that results could just as well have been produced by any method that reduces the compressional modulus in the required amount.

Acknowledgements. This research has been sponsored by the Defense Advanced Research Projects Agency and monitored by the Geophysics Laboratory under contract F19628-87-C-0240. Helpful discussions with S. Day of San Diego State University, J. Murphy of S-CUBED, J. Trulio and N. Perl of Applied Theory, B. Tittmann and J. Bulau of Rockwell International and R. Blandford of DARPA are acknowledged.

REFERENCES

- Ahrens, T. J. and G. E. Duvall, Stress relaxation behind elastic shock waves in rocks, *J. Geophys. Res.* 71, 4349, 1966.
- Aki, K. and P. G. Richards, *Quantitative Seismology Theory and Methods*, W. H. Freeman and Co., San Francisco, p 170-182, 1980.
- Day, S. M. and J. B. Minster, Numerical simulation of attenuated wavefields using a Padé approximate method, *Geophys. J. R. Astr. Soc.* 78, 105, 1984.
- Denny, M. D., A case study of the seismic source function: Salmon and Sterling reevaluated, UCRL-99069 Preprint, Lawrence Livermore National Laboratory, 1989.

- Langston, C. A., Kinematics analysis of strong motion P and SV waves from the Sterling event, *J. Geophys. Res.* 88, 3486, 1983.
- Gupta, I. N., and McLaughlin, K. L., Strain and frequency dependent attenuation estimates in salt from Salmon and Sterling near-field recordings, *Bull. Seis. Soc. Am.* 79, 1111, 1989.
- Kjartansson, E., Constant Q-wave propagation and attenuation, *J. Geophys. Res.* 84, 4737, 1980.
- Larson, D. B., Inelastic wave propagation in sodium chloride, *Bull. Seis. Soc. Am.* 72, 2107, 1982.
- Masse, R. P., Review of seismic source models for underground nuclear explosions, *Bull. Seis. Soc. Am.* 71, 1249, 1981.
- McCartor, G. D. and W. R. Wortman, Experimental and analytic characterization of nonlinear seismic attenuation, MRC-R-900, Mission Research Corporation, Santa Barbara, CA, 1985.
- McCartor, G. D. and W. R. Wortman, Nonlinear attenuation mechanisms in salt at moderate strain based on Salmon data, AFGL-TR-89-0013, Mission Research Corporation, Santa Barbara, CA, 1988. ADA207540
- Minster, J. B. and S. M. Day, Decay of wave fields near an explosive source due to high-strain nonlinear attenuation, *J. Geophys. Res.* 91, 2113, 1986.
- Mueller R. A. and J. R. Murphy, Seismic characteristics of underground nuclear detonations, *Bull. Seis. Soc. Am.*, 61, 1975, 1971.
- Murphey, B. F., Particle motions near explosions in halite, *J. Geophys. Res.* 66, 947, 1961.
- Perret, W. R., Free-field particle motion from a nuclear explosion in salt, Part I, Project Dribble, Salmon Event, VUF-3012, Sandia Laboratory, 1967.
- Rimer, N. and J. T. Cherry, Ground motion predictions for the Grand Saline experiment, S-Cubed Corporation, La Jolla, CA USC-TR-82-25, 1982.

Rogers, L. A., Free-field motion near a nuclear explosion in salt: Project Salmon, *J. Geophys. Res.*, 71, 3415, 1966.

Taylor, J. W. and M. H. Rice, Elastic-plastic properties of iron, *J. Appl. Phys.* 34, 364, 1963.

Tittmann, B. R., Studies of absorption in salt, SC5320SRF, Rockwell International Science Center, Thousand Oaks, CA, 1983.

Trulio, J., Simple scaling and nuclear monitoring, ATR-78-45-1, Applied Theory, Inc., Los Angeles, CA, 1978.

Von Seggern, D. and Blandford, R., Source time functions and spectra for underground nuclear explosions, *J. R. Astr. Soc.*, 31, 83, 1972.

Wilkins, M. L., Calculation of elastic-plastic flow, *Methods in Computational Physics*, Vol 3, 1964.

G. D. McCartor and W. R. Wortman, Mission Research Corporation, P.O. Drawer 719, Santa Barbara, CA 93102.

APPENDIX

Day and Minster [1984] have shown how to include an arbitrary linear Q function in time stepping calculations. For an absorption band an analytic solution is available. An outline of their methods, as generalized to the spherical case is given here.

For a single normalized relaxation function, $m(t)$, the stresses and strains are related by

$$\Sigma_r = (\lambda + 2\mu) \int m(t - \tau) \epsilon_1(\tau) d\tau + 2\lambda \int m(t - \tau) \epsilon_2(\tau) d\tau \quad (A - 1)$$

$$\Sigma_\theta = (2\lambda + 2\mu) \int m(t - \tau) \epsilon_2(\tau) d\tau + \lambda \int m(t - \tau) \epsilon_1(\tau) d\tau \quad (A - 2)$$

Here the strains are

$$\epsilon_1 = \frac{\partial u}{\partial r} \quad (A - 3)$$

$$\epsilon_2 = \frac{u}{r} \quad (A - 4)$$

where u is displacement. Generally one could have two different relaxation functions (e.g., bulk and shear) but we shall not consider this possibility. The λ and μ are the usual Lamé constants which are now the unrelaxed or high-frequency moduli of the medium. The stresses can be written in terms of Q corrected strains, e , as

$$\Sigma_r = (\lambda + 2\mu) e_1 + 2\lambda e_2 \quad (A - 5)$$

$$\Sigma_\theta = (2\lambda + 2\mu)e_2 + \lambda e_1 \quad (\text{A} - 6)$$

Day and Minster have shown how to express the e_i in terms of the ϵ_i

$$e_i = \int m(t - \tau) \epsilon_i d\tau \quad (\text{A} - 7)$$

using a sequence of m Padé approximants to write the integral equation as a differential relation. For an absorption band attenuation with relaxation times between τ_1 and τ_2 and with a flat spectrum, they show that the integral relation can be replaced by

$$e_i(t) = \epsilon_i(t) - \sum_{k=1}^m \zeta_i^k(t) \quad (\text{A} - 8)$$

where

$$\frac{d}{dt} \zeta_i^k + \nu_k \zeta_i^k = \left(\frac{\tau_1^{-1} - \tau_2^{-1}}{\pi} W_k Q_0^{-1} \right) \epsilon_i(t) \quad k = 1, \dots, m \quad (\text{A} - 9)$$

Here Q_0 is the target Q in the absorption band, the

$$\nu_k = \frac{1}{2} \left[\ell_k (\tau_1^{-1} - \tau_2^{-1}) + (\tau_1^{-1} + \tau_2^{-1}) \right] \quad (\text{A} - 10)$$

where the ℓ_k are the abscissas and W_k are the weights for m -point Gauss-Legendre quadrature. The index m is that of the Padé approximant. As m increases, the solution converges to the analytic result which in the frequency-domain is

$$i\omega \tilde{m}(\omega) = \tilde{m}(\omega) = 1 - \frac{2}{\pi Q_0} \ell_n \left[\frac{\tau_2}{\tau_1} \left(\frac{1 + \omega^2 \tau_1^2}{1 + \omega^2 \tau_2^2} \right)^{1/2} \right] + \frac{2i}{\pi Q_0} \tan^{-1} \left(\frac{\omega(\tau_2 - \tau_1)}{1 + \omega^2 \tau_1 \tau_2} \right) \quad (\text{A} - 11)$$

Table 1. Salmon records used including range, ratio of spherical to cylindrical radius and peak velocity.

Record	Range	V_R/V_r	$V_{R_{peak}}$ (m/s)
E-14C-27-AR	166	1.0	13.8
E-14C-22-UR	225	1.36	8.0
E-14 -20-AR	276	1.61	5.1
E- 6 -27-AR	318	1.0	3.75
E-14C-39-AR	402	2.4	2.5
E-11 -34-AR	660	1.06	1.1

FIGURE CAPTIONS

Figure

1. Peak particle velocities from explosions in salt, from Larson [1982].
2. Corrected Salmon velocity records at 166, 225, 276, 402 and 660 meters.
3. Salmon velocity records normalized to unit peak amplitude.
4. Estimate of $Q(f)$ between ranges of 166 and 225 meters.
5. Estimate of $Q(f)$ between ranges of 402 and 660 meters.
6. Estimate of $Q(f)$ between the extreme record pair of 166 and 660 meters.
7. Scaled pulse shapes for a frequency independent Q of 10.
8. Scaled pulse shapes for a specific frequency dependent $Q(f)$.
9. Pulses at Salmon ranges for finite difference calculation of partial shear failure at compressional strain threshold of 10^{-4} .
10. Pulses at Salmon ranges for finite difference calculation of partial shear failure at compressional strain threshold of 10^{-4} and a linear Q of 10.
11. Pulses at Salmon ranges for finite difference calculation of distributed partial shear failure and a linear Q of 10.

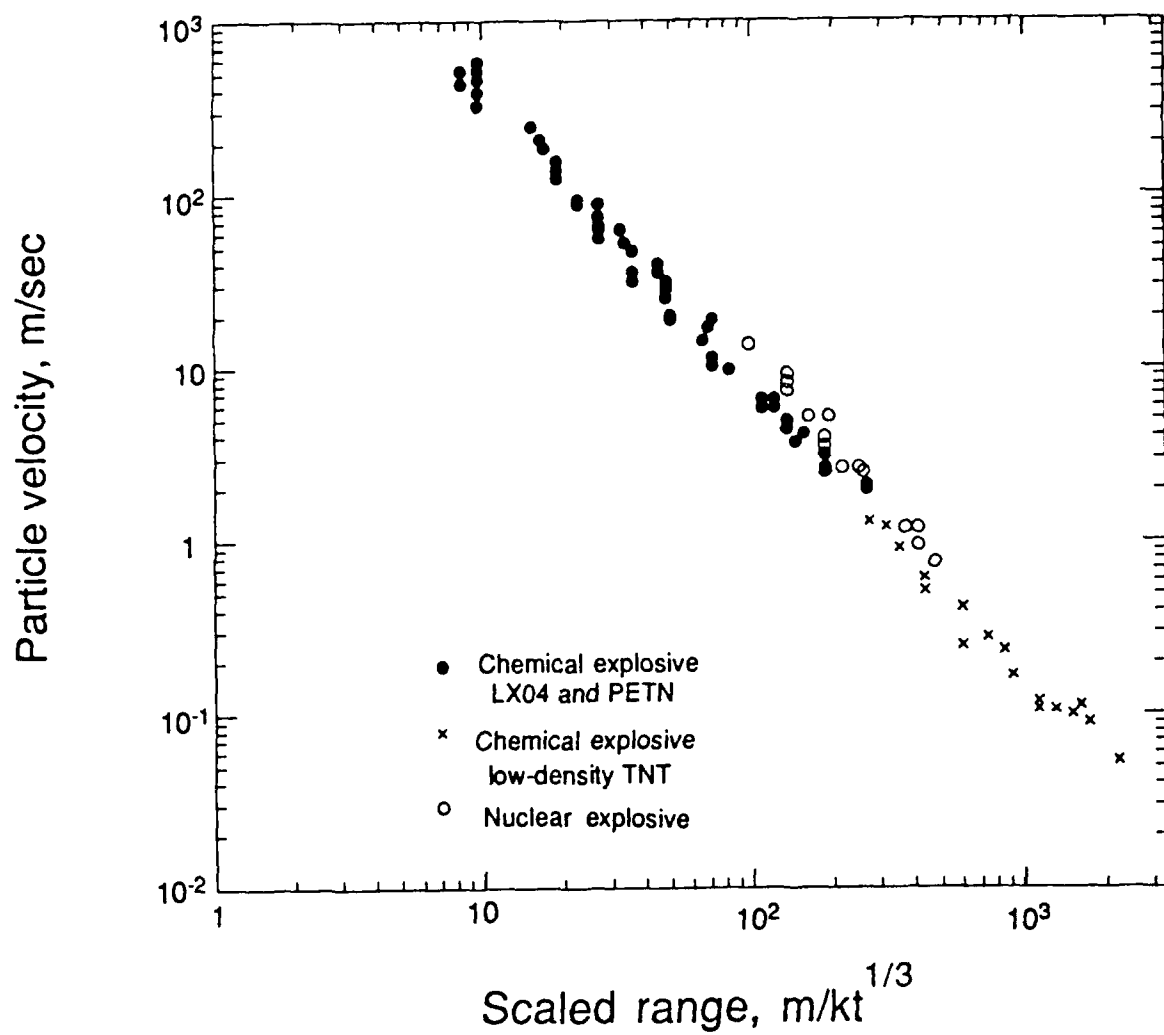


Figure 1. Peak particle velocities from explosions in salt, from Larson [1982].

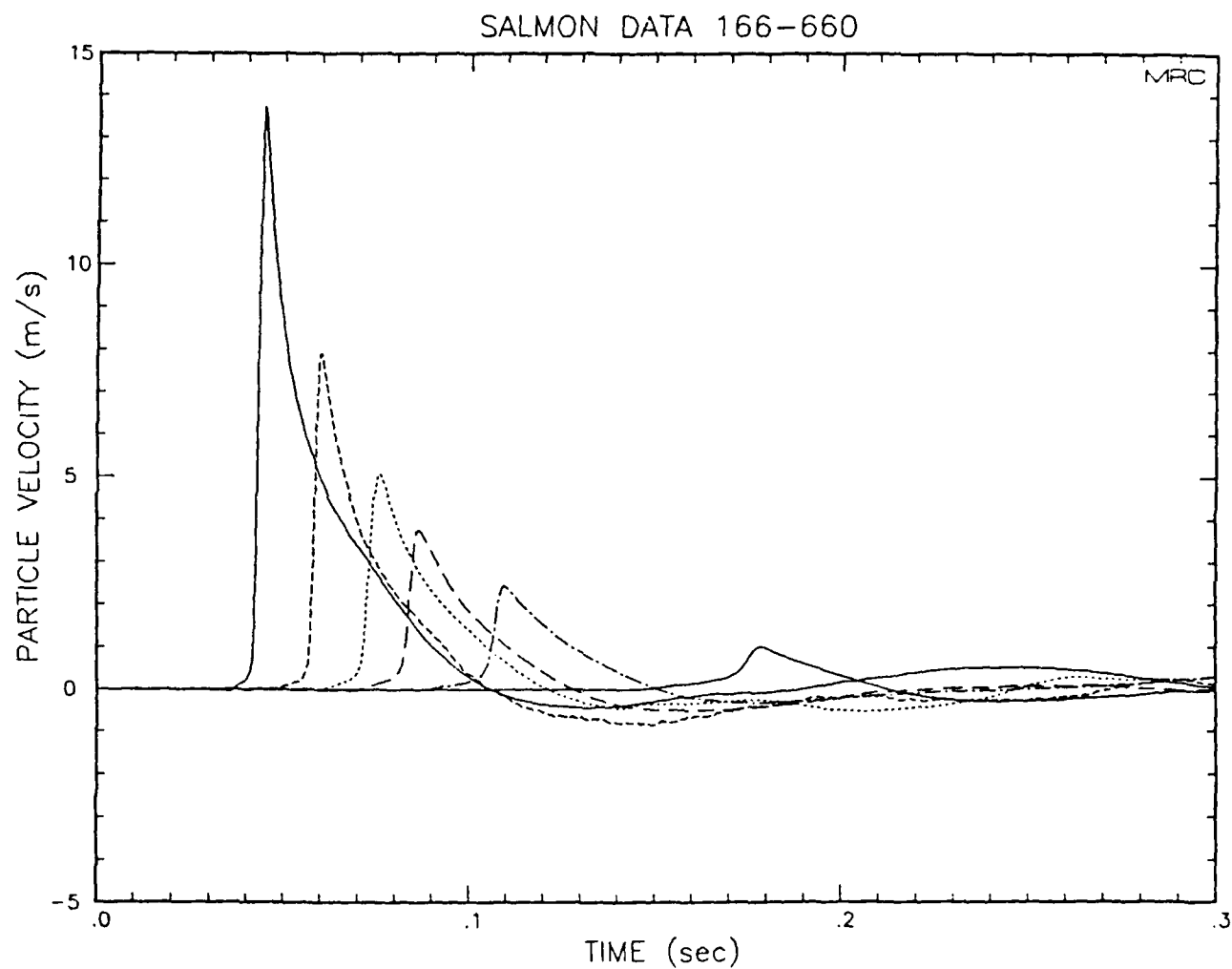


Figure 2. Corrected Salmon velocity records at 166, 225, 276, 402 and 660 meters.

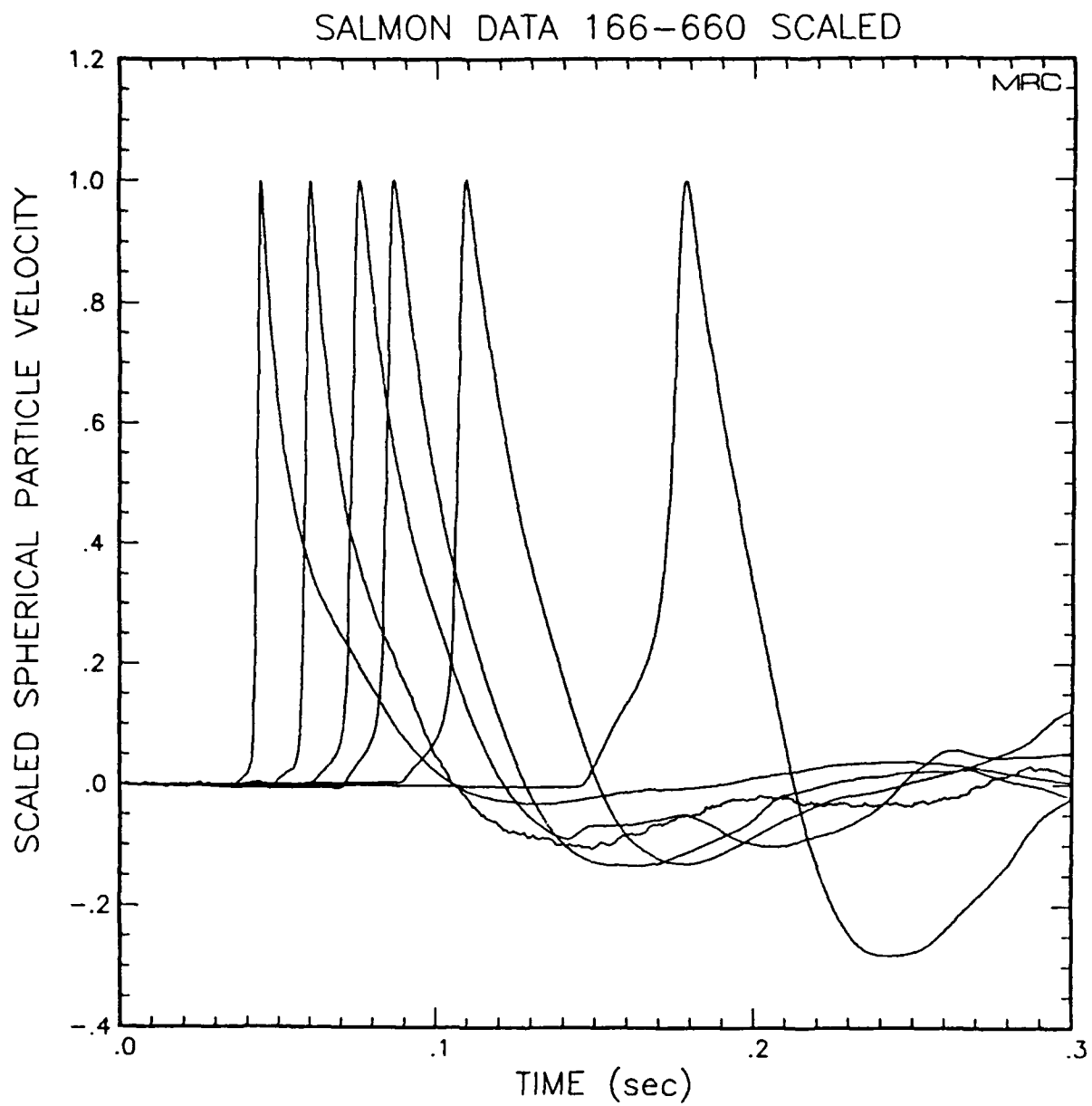


Figure 3. Salmon velocity records normalized to unit peak amplitude.

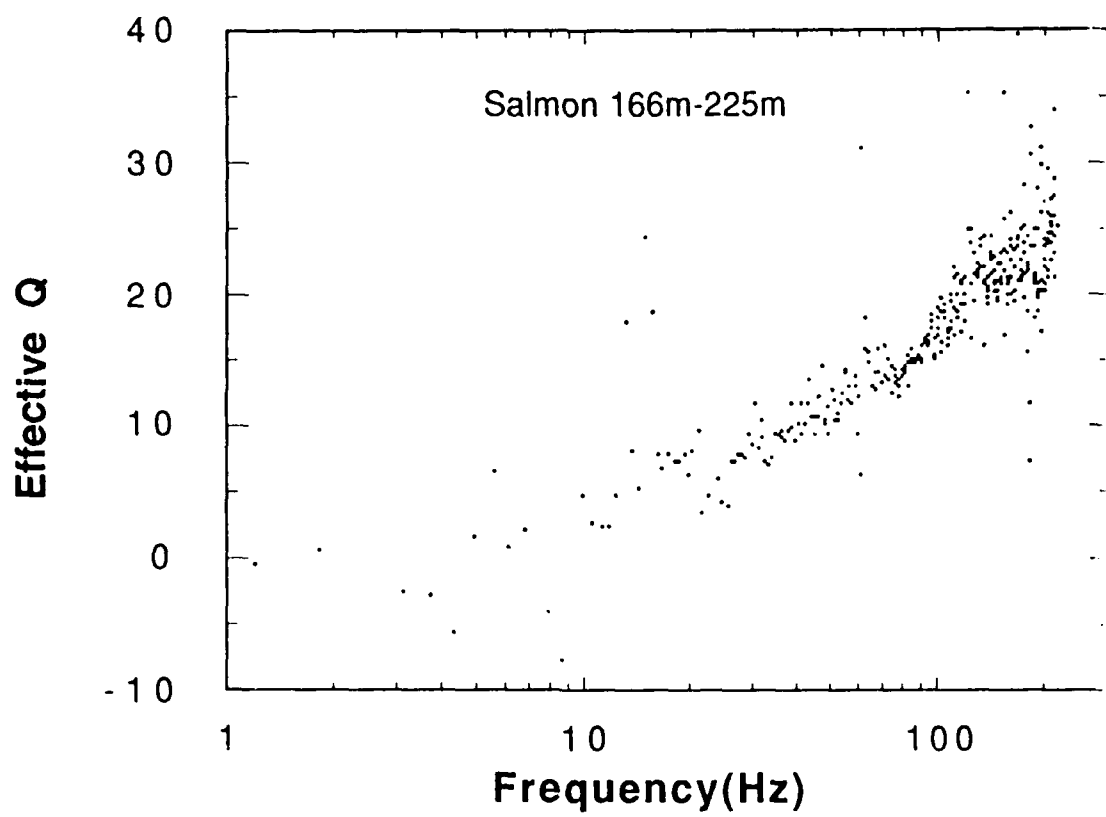


Figure 4. Estimate of $Q(f)$ between ranges of 166 and 225 meters.

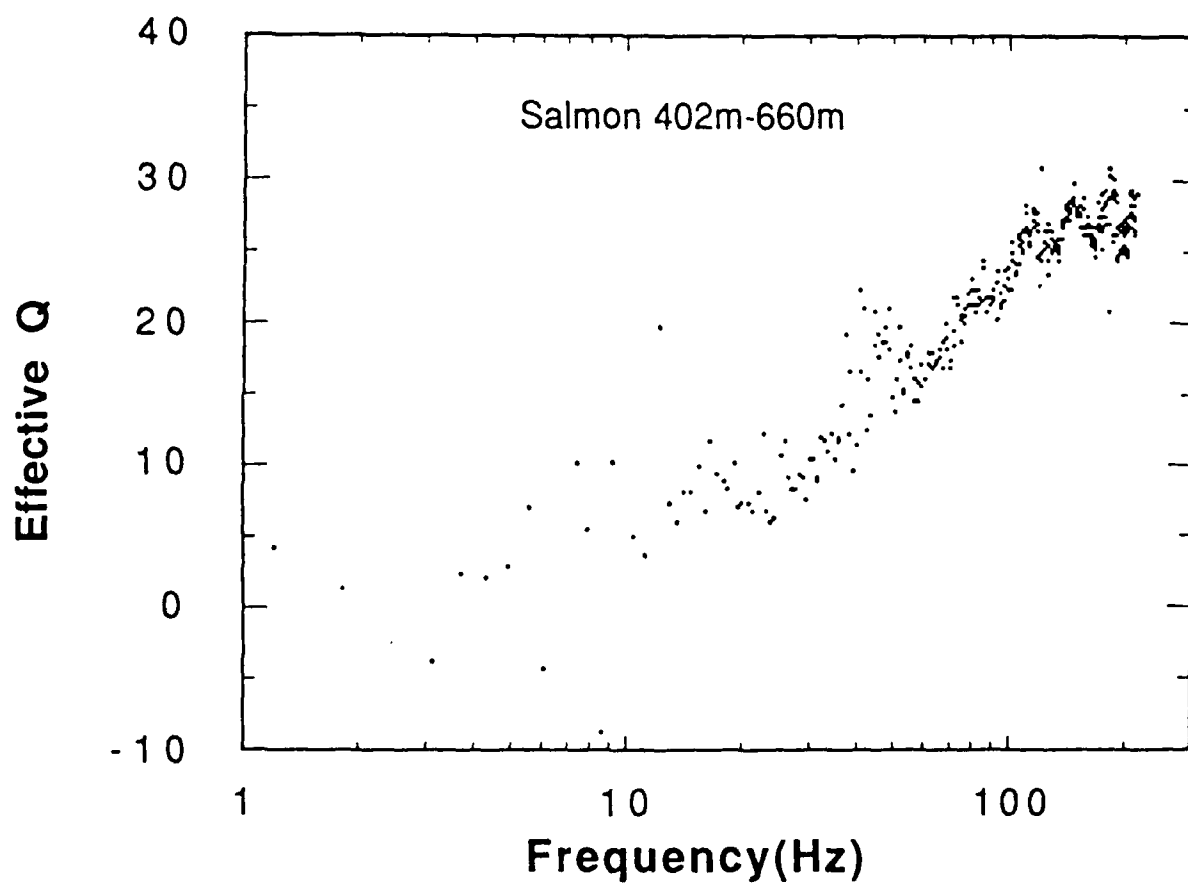


Figure 5. Estimate of $Q(f)$ between ranges of 402 and 660 meters.

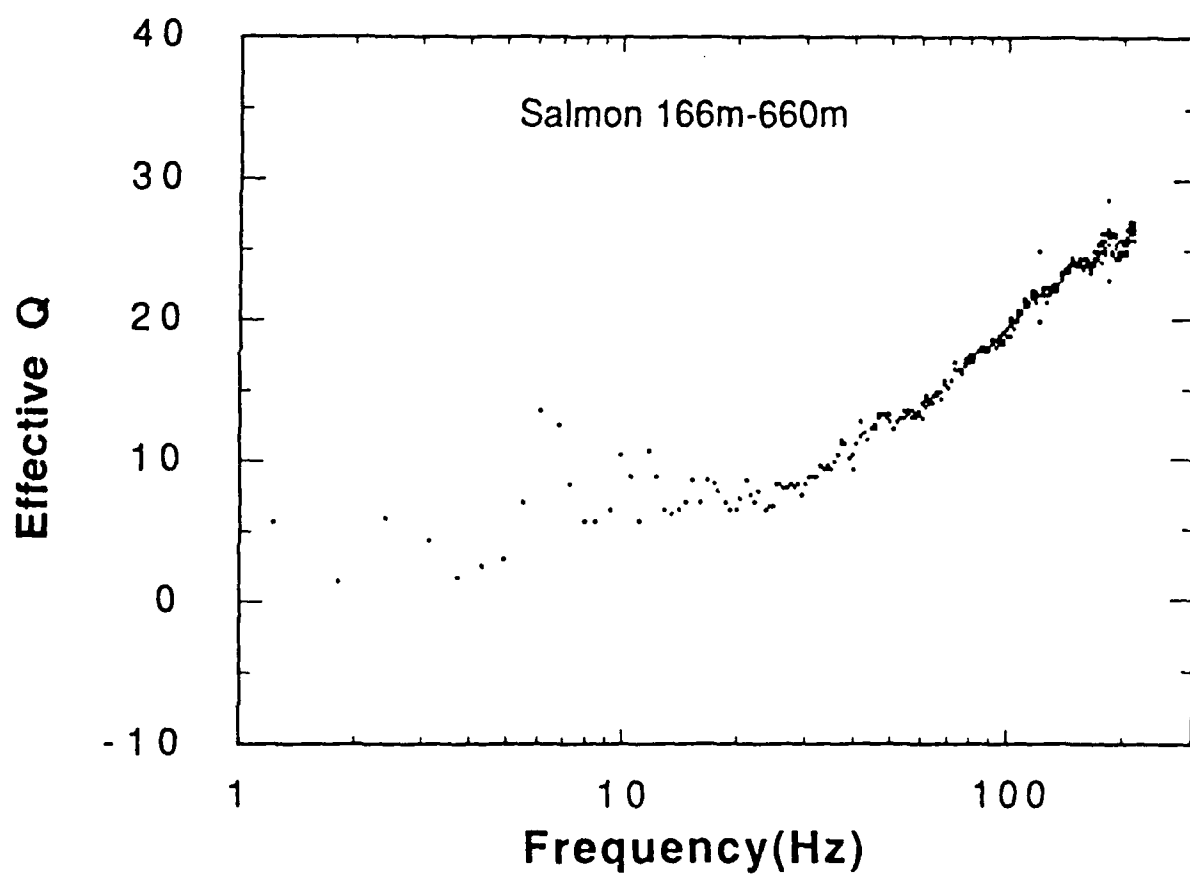


Figure 6. Estimate of $Q(f)$ between the extreme record pair of 166 and 660 meters.

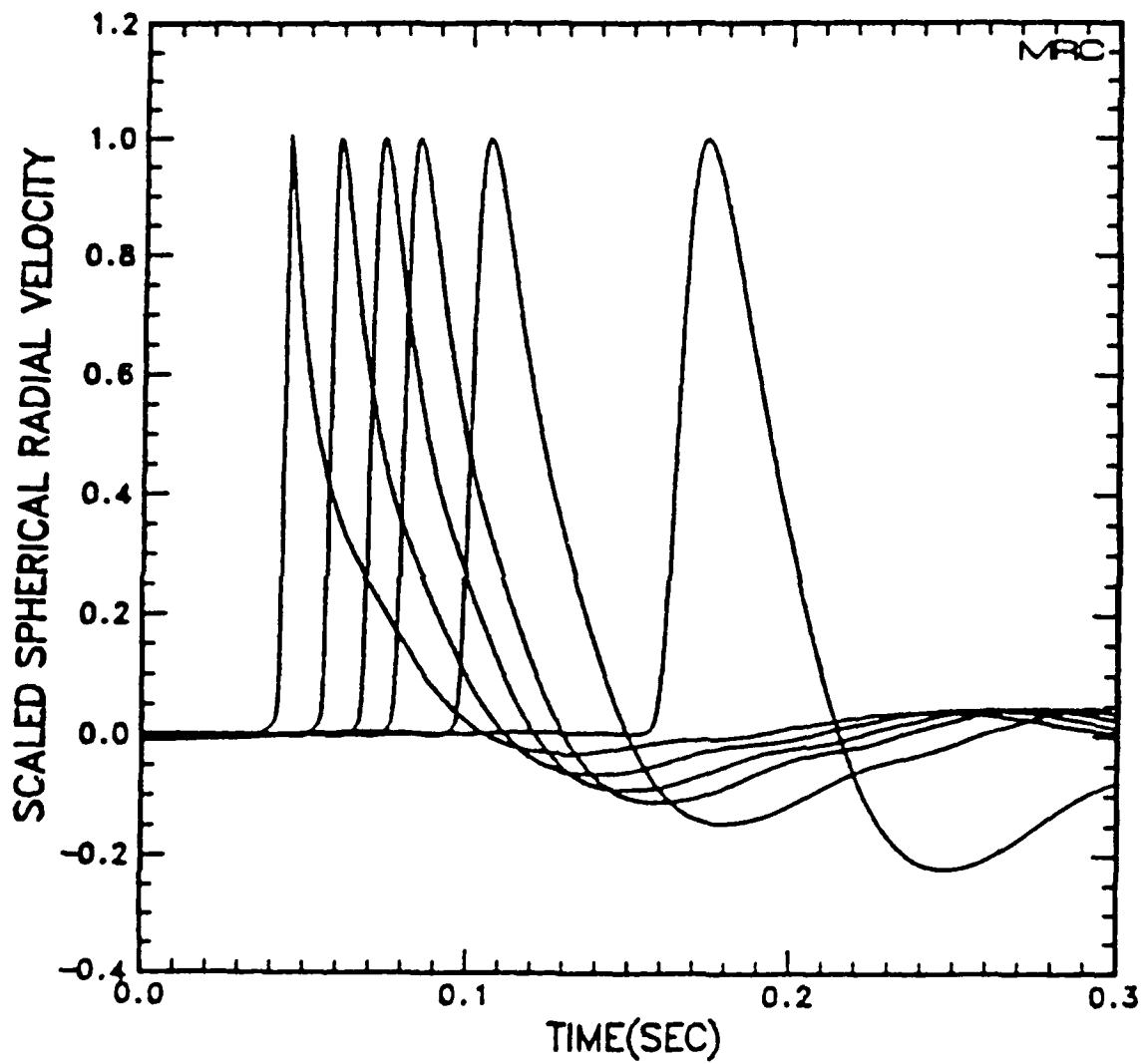


Figure 7. Scaled pulse shapes for a frequency independent Q of 10.

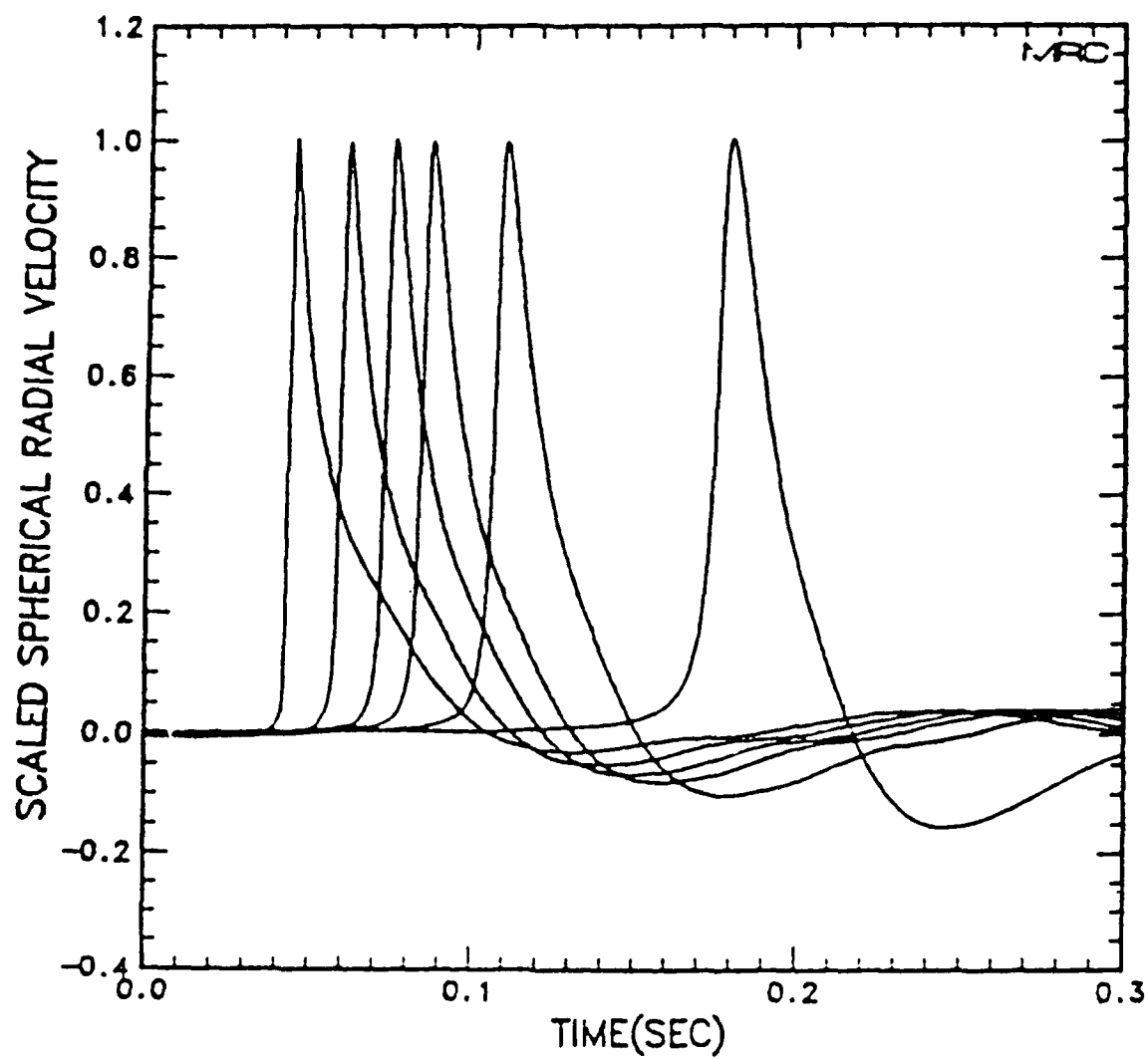


Figure 8. Scaled pulse shapes for a specific frequency dependent $Q(f)$.

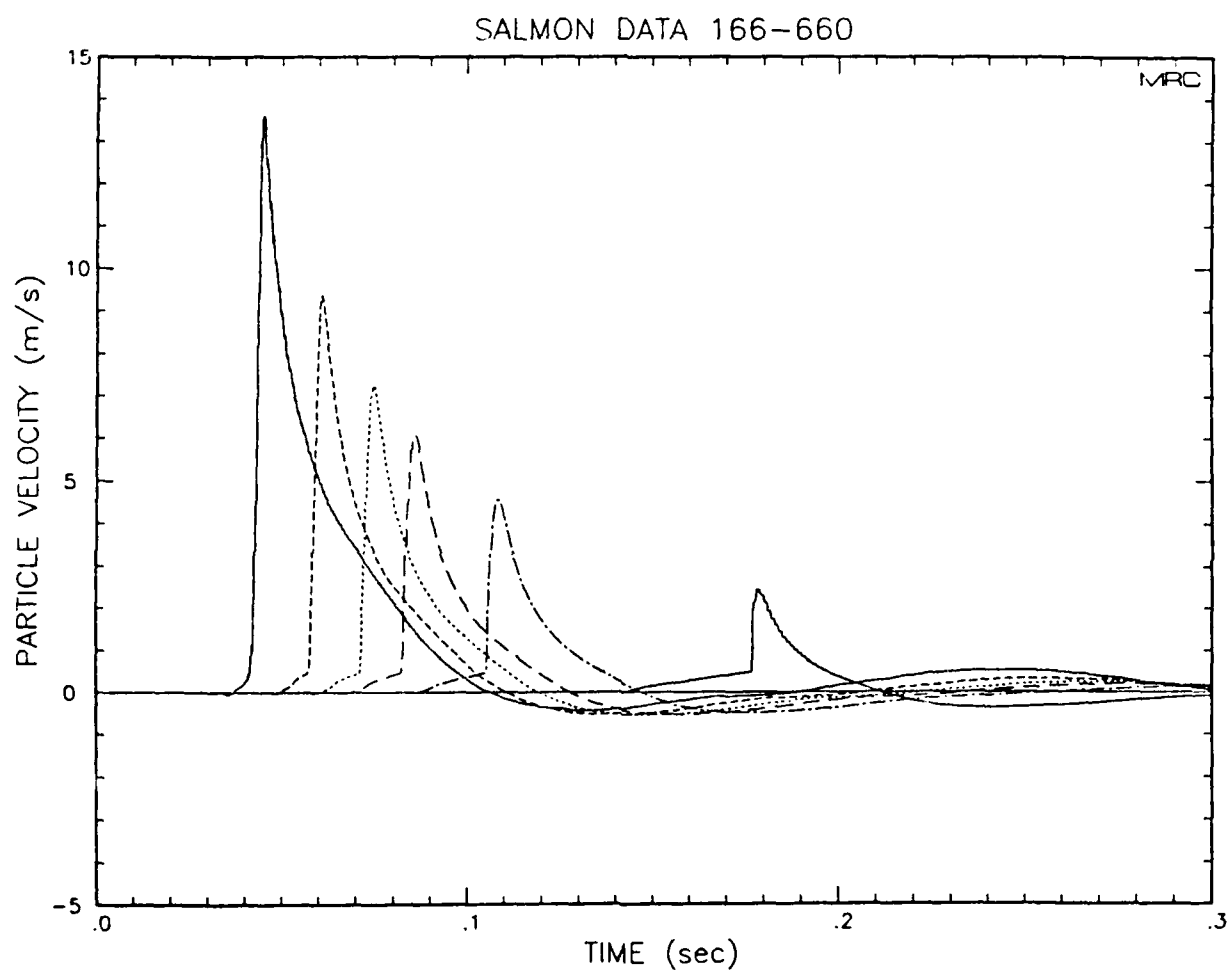


Figure 9. Pulses at Salmon ranges for finite difference calculation of partial shear failure at compressional strain threshold of 10^{-4} .

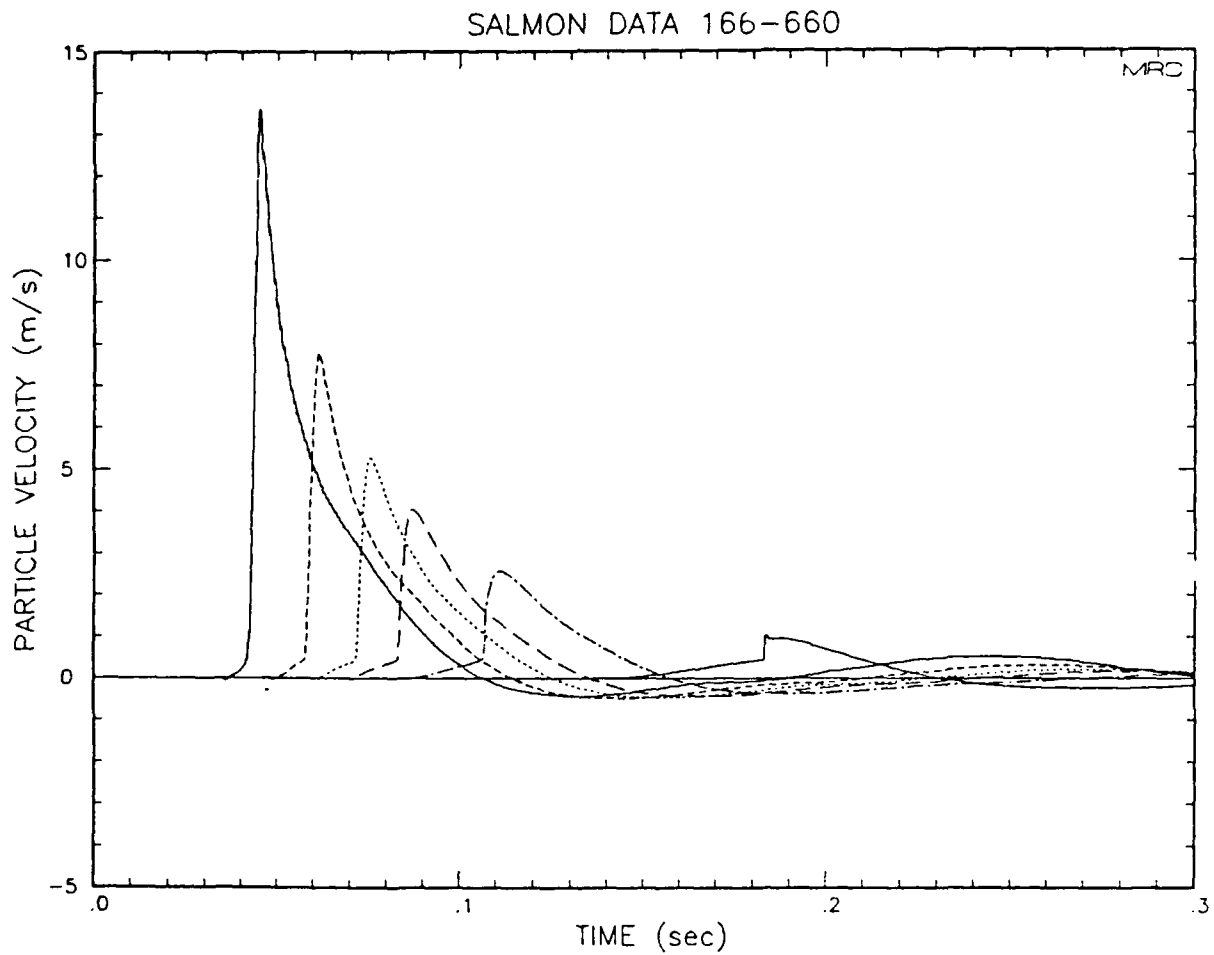


Figure 10. Pulses at Salmon ranges for finite difference calculation of partial shear failure at compressional strain threshold of 10^{-4} and a linear Q of 10. 34

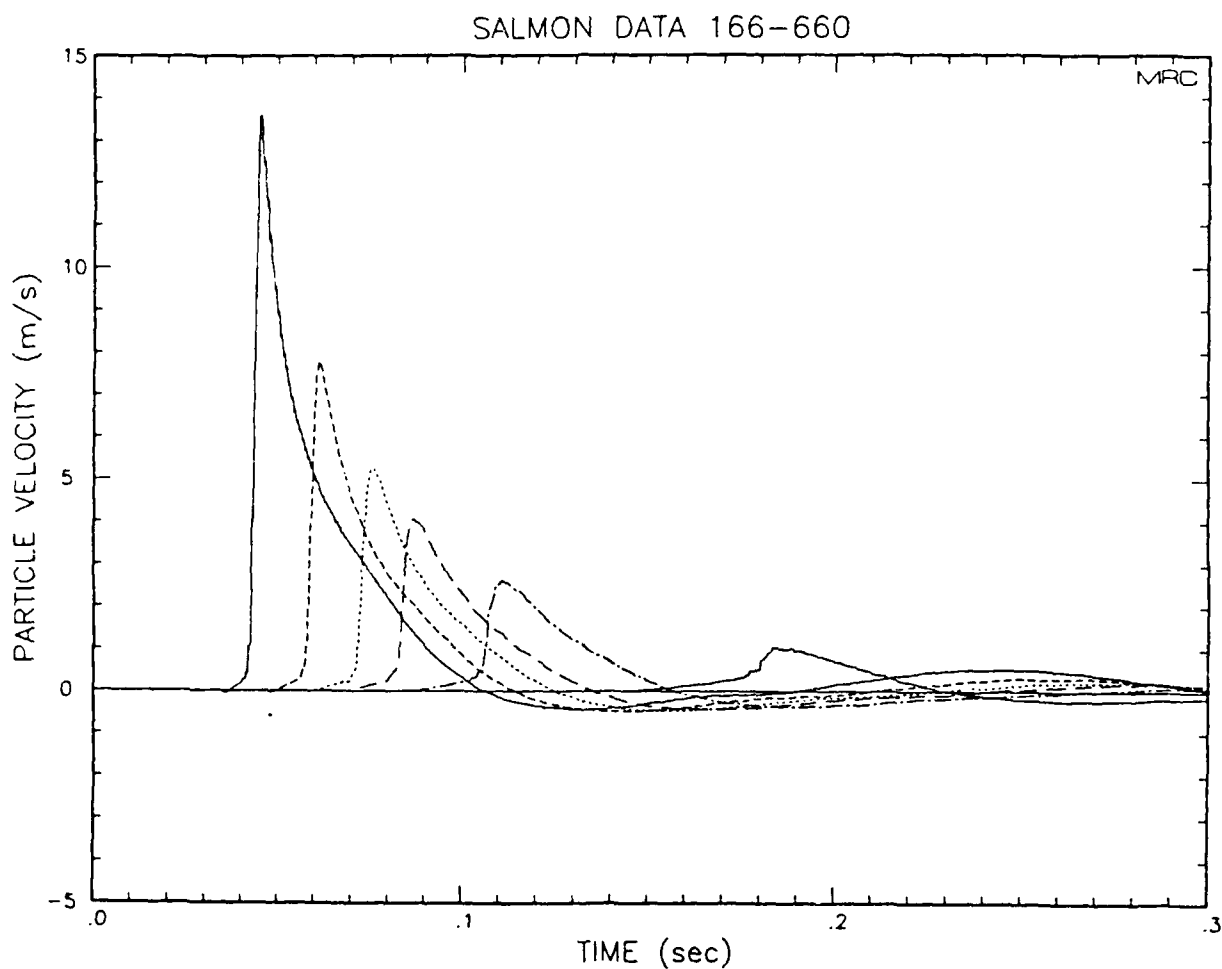


Figure 11. Pulses at Salmon ranges for finite difference calculation of distributed partial shear failure and a linear Q of 10.

Prof. Thomas Ahrens
Seismological Lab, 252-21
Division of Geological & Planetary Sciences
California Institute of Technology
Pasadena, CA 91125

Prof. Charles B. Archambeau
CIRES
University of Colorado
Boulder, CO 80309

Prof. Muawia Barazangi
Institute for the Study of the Continent
Cornell University
Ithaca, NY 14853

Dr. Douglas R. Baumgardt
ENSCO, Inc
5400 Port Royal Road
Springfield, VA 22151-2388

Prof. Jonathan Berger
IGPP, A-025
Scripps Institution of Oceanography
University of California, San Diego
La Jolla, CA 92093

Dr. Lawrence J. Burdick
Woodward-Clyde Consultants
566 El Dorado Street
Pasadena, CA 91109-3245

Dr. Karl Coyner
New England Research, Inc.
76 Olcott Drive
White River Junction, VT 05001

Prof. Vernon F. Cormier
Department of Geology & Geophysics
U-45, Room 207
The University of Connecticut
Storrs, CT 06268

Prof. Steven Day
Department of Geological Sciences
San Diego State University
San Diego, CA 92182

Dr. Zoltan A. Der
ENSCO, Inc.
5400 Port Royal Road
Springfield, VA 22151-2388

Prof. John Ferguson
Center for Lithospheric Studies
The University of Texas at Dallas
P.O. Box 830688
Richardson, TX 75083-0688

Prof. Stanley Flotte
Applied Sciences Building
University of California
Santa Cruz, CA 95064

Dr. Alexander Florence
SRI International
333 Ravenswood Avenue
Menlo Park, CA 94025-3493

Prof. Henry L. Gray
Vice Provost and Dean
Department of Statistical Sciences
Southern Methodist University
Dallas, TX 75275

Dr. Indra Gupta
Teledyne Geotech
314 Montgomery Street
Alexandria, VA 22314

Prof. David G. Harkrider
Seismological Laboratory
Division of Geological & Planetary Sciences
California Institute of Technology
Pasadena, CA 91125

Prof. Donald V. Helmberger
Seismological Laboratory
Division of Geological & Planetary Sciences
California Institute of Technology
Pasadena, CA 91125

Prof. Eugene Herrin
Institute for the Study of Earth and Man
Geophysical Laboratory
Southern Methodist University
Dallas, TX 75275

Prof. Robert B. Herrmann
Department of Earth & Atmospheric Sciences
St. Louis University
St. Louis, MO 63156

Prof. Bryan Isacks
Cornell University
Department of Geological Sciences
SNEE Hall
Ithaca, NY 14850

Dr. Rong-Song Jih
Teledyne Geotech
314 Montgomery Street
Alexandria, VA 22314

Prof. Lane R. Johnson
Seismographic Station
University of California
Berkeley, CA 94720

Prof. Alan Kafka
Department of Geology & Geophysics
Boston College
Chestnut Hill, MA 02167

Prof. Fred K. Lamb
University of Illinois at Urbana-Champaign
Department of Physics
1110 West Green Street
Urbana, IL 61801

Prof. Charles A. Langston
Geosciences Department
403 Deike Building
The Pennsylvania State University
University Park, PA 16802

Prof. Thome Lay
Department of Geological Sciences
1006 C.C. Little Building
University of Michigan
Ann Arbor, MI 48109-1063

Prof. Arthur Lerner-Lam
Lamont-Doherty Geological Observatory
of Columbia University
Palisades, NY 10964

Dr. Christopher Lynnes
Teledyne Geotech
314 Montgomery Street
Alexandria, VA 22314

Prof. Peter Malin
University of California at Santa Barbara
Institute for Crustal Studies
Santa Barbara, CA 93106

Dr. Randolph Martin, III
New England Research, Inc.
76 Olcott Drive
White River Junction, VT 05001

Dr. Gary McCartor
Mission Research Corporation
735 State Street
P.O. Drawer 719
Santa Barbara, CA 93102 (2 copies)

Prof. Thomas V. McEvilly
Seismographic Station
University of California
Berkeley, CA 94720

Dr. Keith L. McLaughlin
S-CUBED
A Division of Maxwell Laboratory
P.O. Box 1620
La Jolla, CA 92038-1620

Prof. William Menke
Lamont-Doherty Geological Observatory
of Columbia University
Palisades, NY 10964

Stephen Miller
SRI International
333 Ravenswood Avenue
Box AF 116
Menlo Park, CA 94025-3493

Prof. Bernard Minster
IGPP, A-025
Scripps Institute of Oceanography
University of California, San Diego
La Jolla, CA 92093

Prof. Brian J. Mitchell
Department of Earth & Atmospheric Sciences
St. Louis University
St. Louis, MO 63156

Mr. Jack Murphy
S-CUBED, A Division of Maxwell Laboratory
11800 Sunrise Valley Drive
Suite 1212
Reston, VA 22091 (2 copies)

Dr. Bao Nguyen
GL/LWH
Hanscom AFB, MA 01731-5000

Prof. John A. Orcutt
IGPP, A-025
Scripps Institute of Oceanography
University of California, San Diego
La Jolla, CA 92093

Prof. Keith Priestley
University of Nevada
Mackay School of Mines
Reno, NV 89557

Prof. Paul G. Richards
Lamont-Doherty Geological Observatory
of Columbia University
Palisades, NY 10964

Dr. Wilmer Rivers
Teledyne Geotech
314 Montgomery Street
Alexandria, VA 22314

Dr. Alan S. Ryall, Jr.
Center for Seismic Studies
1300 North 17th Street
Suite 1450
Arlington, VA 22209-2308

Prof. Charles G. Sammis
Center for Earth Sciences
University of Southern California
University Park
Los Angeles, CA 90089-0741

Prof. Christopher H. Scholz
Lamont-Doherty Geological Observatory
of Columbia University
Palisades, NY 10964

Prof. David G. Simpson
Lamont-Doherty Geological Observatory
of Columbia University
Palisades, NY 10964

Dr. Jeffrey Stevens
S-CUBED
A Division of Maxwell Laboratory
P.O. Box 1620
La Jolla, CA 92038-1620

Prof. Brian Stump
Institute for the Study of Earth & Man
Geophysical Laboratory
Southern Methodist University
Dallas, TX 75275

Prof. Jeremiah Sullivan
University of Illinois at Urbana-Champaign
Department of Physics
1110 West Green Street
Urbana, IL 61801

Prof. Clifford Thurber
University of Wisconsin-Madison
Department of Geology & Geophysics
1215 West Dayton Street
Madison, WS 53706

Prof. M. Nafi Toksoz
Earth Resources Lab
Massachusetts Institute of Technology
42 Carleton Street
Cambridge, MA 02142

Prof. John E. Vidale
University of California at Santa Cruz
Seismological Laboratory
Santa Cruz, CA 95064

Prof. Terry C. Wallace
Department of Geosciences
Building #77
University of Arizona
Tucson, AZ 85721

Dr. Raymond Willeman
GL/LWH
Hanscom AFB, MA 01731-5000

Dr. Lorraine Wolf
GL/LWH
Hanscom AFB, MA 01731-5000

Prof. Francis T. Wu
Department of Geological Sciences
State University of New York
at Binghamton
Vestal, NY 13901

OTHERS (United States)

Dr. Monem Abdel-Gawad
Rockwell International Science Center
1049 Camino Dos Rios
Thousand Oaks, CA 91360

Dr. Stephen Bratt
Science Applications Int'l Corp.
10210 Campus Point Drive
San Diego, CA 92121

Prof. Keiiti Aki
Center for Earth Sciences
University of Southern California
University Park
Los Angeles, CA 90089-0741

Michael Browne
Teledyne Geotech
3401 Shiloh Road
Garland, TX 75041

Prof. Shelton S. Alexander
Geosciences Department
403 Deike Building
The Pennsylvania State University
University Park, PA 16802

Mr. Roy Burger
1221 Serry Road
Schenectady, NY 12309

Dr. Ralph Archuleta
Department of Geological Sciences
University of California at Santa Barbara
Santa Barbara, CA 93102

Dr. Robert Burrige
Schlumberger-Doll Research Center
Old Quarry Road
Ridgefield, CT 06877

Dr. Thomas C. Bache, Jr.
Science Applications Int'l Corp.
10210 Campus Point Drive
San Diego, CA 92121 (2 copies)

Dr. Jerry Carter
Rondout Associates
P.O. Box 224
Stone Ridge, NY 12484

J. Barker
Department of Geological Sciences
State University of New York
at Binghamton
Vestal, NY 13901

Dr. W. Winston Chan
Teledyne Geotech
314 Montgomery Street
Alexandria, VA 22314-1581

Dr. T.J. Bennett
S-CUBED
A Division of Maxwell Laboratory
11800 Sunrise Valley Drive, Suite 1212
Reston, VA 22091

Dr. Theodore Cherry
Science Horizons, Inc.
710 Encinitas Blvd., Suite 200
Encinitas, CA 92024 (2 copies)

Mr. William J. Best
907 Westwood Drive
Vienna, VA 22180

Prof. Jon F. Claerbout
Department of Geophysics
Stanford University
Stanford, CA 94305

Dr. N. Biswas
Geophysical Institute
University of Alaska
Fairbanks, AK 99701

Prof. Robert W. Clayton
Seismological Laboratory
Division of Geological & Planetary Sciences
California Institute of Technology
Pasadena, CA 91125

Dr. G.A. Bollinger
Department of Geological Sciences
Virginia Polytechnical Institute
21044 Derring Hall
Blacksburg, VA 24061

Prof. F. A. Dahlen
Geological and Geophysical Sciences
Princeton University
Princeton, NJ 08544-0636

Prof. Anton W. Dainty
Earth Resources Lab
Massachusetts Institute of Technology
42 Carleton Street
Cambridge, MA 02142

Prof. Adam Dziewonski
Hoffman Laboratory
Harvard University
20 Oxford St
Cambridge, MA 02138

Prof. John Ebel
Department of Geology & Geophysics
Boston College
Chestnut Hill, MA 02167

Eric Fielding
SNEE Hall
INSTOC
Cornell University
Ithaca, NY 14853

Prof. Donald Forsyth
Department of Geological Sciences
Brown University
Providence, RI 02912

Dr. Anthony Gangi
Texas A&M University
Department of Geophysics
College Station, TX 77843

Dr. Freeman Gilbert
Inst. of Geophysics & Planetary Physics
University of California, San Diego
P.O. Box 109
La Jolla, CA 92037

Mr. Edward Giller
Pacific Sierra Research Corp.
1401 Wilson Boulevard
Arlington, VA 22209

Dr. Jeffrey W. Given
Sierra Geophysics
11255 Kirkland Way
Kirkland, WA 98033

Prof. Steven Grand
University of Texas at Austin
Department of Geological Sciences
Austin, TX 78713-7909

Prof. Roy Greenfield
Geosciences Department
403 Deike Building
The Pennsylvania State University
University Park, PA 16802

Dan N. Hagedorn
Battelle
Pacific Northwest Laboratories
Battelle Boulevard
Richland, WA 99352

Kevin Hutchenson
Department of Earth Sciences
St. Louis University
3507 Laclede
St. Louis, MO 63103

Prof. Thomas H. Jordan
Department of Earth, Atmospheric
and Planetary Sciences
Massachusetts Institute of Technology
Cambridge, MA 02139

Robert C. Kemerait
ENSCO, Inc.
445 Pineda Court
Melbourne, FL 32940

William Kikendall
Teledyne Geotech
3401 Shiloh Road
Garland, TX 75041

Prof. Leon Knopoff
University of California
Institute of Geophysics & Planetary Physics
Los Angeles, CA 90024

Prof. L. Timothy Long
School of Geophysical Sciences
Georgia Institute of Technology
Atlanta, GA 30332

Dr. George Mellman
Sierra Geophysics
11255 Kirkland Way
Kirkland, WA 98033

Prof. John Nabelek
College of Oceanography
Oregon State University
Corvallis, OR 97331

Prof. Geza Nagy
University of California, San Diego
Department of Ames, M.S. B-010
La Jolla, CA 92093

Prof. Amos Nur
Department of Geophysics
Stanford University
Stanford, CA 94305

Prof. Jack Oliver
Department of Geology
Cornell University
Ithaca, NY 14850

Prof. Robert Phinney
Geological & Geophysical Sciences
Princeton University
Princeton, NJ 08544-0636

Dr. Paul Pomeroy
Rondout Associates
P.O. Box 224
Stone Ridge, NY 12484

Dr. Jay Pulli
RADIX System, Inc.
2 Taft Court, Suite 203
Rockville, MD 20850

Dr. Norton Rimer
S-CUBED
A Division of Maxwell Laboratory
P.O. Box 1620
La Jolla, CA 92038-1620

Prof. Larry J. Ruff
Department of Geological Sciences
1006 C.C. Little Building
University of Michigan
Ann Arbor, MI 48109-1063

Dr. Richard Sailor
TASC Inc.
55 Walkers Brook Drive
Reading, MA 01867

Thomas J. Sereno, Jr.
Science Application Int'l Corp.
10210 Campus Point Drive
San Diego, CA 92121

John Sherwin
Teledyne Geotech
3401 Shiloh Road
Garland, TX 75041

Prof. Robert Smith
Department of Geophysics
University of Utah
1400 East 2nd South
Salt Lake City, UT 84112

Prof. S. W. Smith
Geophysics Program
University of Washington
Seattle, WA 98195

Dr. Stewart Smith
IRIS Inc.
1616 North Fort Myer Drive
Suite 1440
Arlington, VA 22209

Dr. George Sutton
Rondout Associates
P.O. Box 224
Stone Ridge, NY 12484

Prof. L. Sykes
Lamont-Doherty Geological Observatory
of Columbia University
Palisades, NY 10964

Prof. Pradeep Talwani
Department of Geological Sciences
University of South Carolina
Columbia, SC 29208

Prof. Ta-liang Teng
Center for Earth Sciences
University of Southern California
University Park
Los Angeles, CA 90089-0741

Dr. R.B. Tittmann
Rockwell International Science Center
1049 Camino Dos Rios
P.O. Box 1085
Thousand Oaks, CA 91360

Dr. Gregory van der Vink
IRIS, Inc.
1616 North Fort Myer Drive
Suite 1440
Arlington, VA 22209

William R. Walter
Seismological Laboratory
University of Nevada
Reno, NV 89557

- Dr. Gregory Wojcik
Weidlinger Associates
4410 El Camino Real
Suite 110
• Los Altos, CA 94022

Prof. John H. Woodhouse
Hoffman Laboratory
Harvard University
20 Oxford Street
Cambridge, MA 02138

Dr. Gregory B. Young
ENSCO, Inc.
5400 Port Royal Road
Springfield, VA 22151-2388

FOREIGN (Others)

Dr. Peter Basham
Earth Physics Branch
Geological Survey of Canada
1 Observatory Crescent
Ottawa, Ontario, CANADA K1A 0Y3

Dr. Eduard Berg
Institute of Geophysics
University of Hawaii
Honolulu, HI 96822

Dr. Michel Bouchon
I.R.I.G.M.-B.P. 68
38402 St. Martin D'Herès
Cedex, FRANCE

Dr. Hilmar Bungum
NTNF/NORSAR
P.O. Box 51
N-2007 Kjeller, NORWAY

Dr. Michel Campillo
Observatoire de Grenoble
I.R.I.G.M.-B.P. 53
38041 Grenoble, FRANCE

Dr. Kin Yip Chun
Geophysics Division
Physics Department
University of Toronto
Ontario, CANADA M5S 1A7

Dr. Alan Douglas
Ministry of Defense
Blacknest, Brimpton
Reading RG7-4RS, UNITED KINGDOM

Dr. Roger Hansen
NTNF/NORSAR
P.O. Box 51
N-2007 Kjeller, NORWAY

Dr. Manfred Henger
Federal Institute for Geosciences & Nat'l Res.
Postfach 510153
D-3000 Hanover 51, FRG

Ms. Eva Johannisson
Senior Research Officer
National Defense Research Inst.
P.O. Box 27322
S-102 54 Stockholm, SWEDEN

Dr. Fekadu Kebede
Seismological Section
Box 12019
S-750 Uppsala, SWEDEN

Dr. Tormod Kvaerna
NTNF/NORSAR
P.O. Box 51
N-2007 Kjeller, NORWAY

Dr. Peter Marshal
Procurement Executive
Ministry of Defense
Blacknest, Brimpton
Reading FG7-4RS, UNITED KINGDOM

Prof. Ari Ben-Menahem
Department of Applied Mathematics
Weizman Institute of Science
Rehovot, ISRAEL 951729

Dr. Robert North
Geophysics Division
Geological Survey of Canada
1 Observatory Crescent
Ottawa, Ontario, CANADA K1A 0Y3

Dr. Frode Ringdal
NTNF/NORSAR
P.O. Box 51
N-2007 Kjeller, NORWAY

Dr. Jorg Schlittenhardt
Federal Institute for Geosciences & Nat'l Res.
Postfach 510153
D-3000 Hannover 51, FEDERAL REPUBLIC OF
GERMANY

Prof. Daniel Walker
University of Hawaii
Institute of Geophysics
Honolulu, HI 96822

FOREIGN CONTRACTORS

Dr. Ramon Cabre, S.J.
Observatorio San Calixto
Casilla 5939
La Paz, Bolivia

Prof. Hans-Peter Harjes
Institute for Geophysik
Ruhr University/Bochum
P.O. Box 102148
4630 Bochum 1, FRG

Prof. Eystein Husebye
NTNF/NORSAR
P.O. Box 51
N-2007 Kjeller, NORWAY

Prof. Brian L.N. Kennett
Research School of Earth Sciences
Institute of Advanced Studies
G.P.O. Box 4
Canberra 2601, AUSTRALIA

Dr. Bernard Massinon
Societe Radiomana
27 rue Claude Bernard
75005 Paris, FRANCE (2 Copies)

Dr. Pierre Mecheler
Societe Radiomana
27 rue Claude Bernard
75005 Paris, FRANCE

Dr. Svein Mykkeltveit
NTNF/NORSAR
P.O. Box 51
N-2007 Kjeller, NORWAY

GOVERNMENT

Dr. Ralph Alewine III
DARPA/NMRC
1400 Wilson Boulevard
Arlington, VA 22209-2308

Mr. James C. Battis
GL/LWH
Hanscom AFB, MA 01731-5000

Dr. Robert Blandford
DARPA/NMRO
1400 Wilson Boulevard
Arlington, VA 22209-2308

Eric Chael
Division 9241
Sandia Laboratory
Albuquerque, NM 87185

Dr. John J. Cipar
GL/LWH
Hanscom AFB, MA 01731-5000

Mr. Charles L. Taylor
GL/LWH
Hanscom AFB, MA 01731-5000

Dr. Jack Evernden
USGS - Earthquake Studies
345 Middlefield Road
Menlo Park, CA 94025

Art Frankel
USGS
922 National Center
Reston, VA 22092

Dr. T. Hanks
USGS
Nat'l Earthquake Research Center
345 Middlefield Road
Menlo Park, CA 94025

Dr. James Hannon
Lawrence Livermore Nat'l Laboratory
P.O. Box 808
Livermore, CA 94550

Paul Johnson
ESS-4, Mail Stop J979
Los Alamos National Laboratory
Los Alamos, NM 87545

Janet Johnston
GL/LWH
Hanscom AFB, MA 01731-5000

Dr. Katharine Kadinsky-Cade
GL/LWH
Hanscom AFB, MA 01731-5000

Ms. Ann Kerr
IGPP, A-025
Scripps Institute of Oceanography
University of California, San Diego
La Jolla, CA 92093

Dr. Max Koontz
US Dept of Energy/DP 5
Forrestal Building
1000 Independence Avenue
Washington, DC 20585

Dr. W.H.K. Lee
Office of Earthquakes, Volcanoes,
& Engineering
345 Middlefield Road
Menlo Park, CA 94025

Dr. William Leith
U.S. Geological Survey
Mail Stop 928
Reston, VA 22092

Dr. Richard Lewis
Director, Earthquake Engineering & Geophysics
U.S. Army Corps of Engineers
Box 631
Vicksburg, MS 39180

James F. Lewkowicz
GL/LWH
Hanscom AFB, MA 01731-5000

Mr. Alfred Lieberman
ACDA/VI-OA State Department Bldg
Room 5726
320 - 21st Street, NW
Washington, DC 20451

Stephen Mangino
GL/LWH
Hanscom AFB, MA 01731-5000

Dr. Frank F. Pilotte
HQ AFTAC/IT
Patrick AFB, FL 32925-6001

Dr. Robert Masse
Box 25046, Mail Stop 967
Denver Federal Center
Denver, CO 80225

Mr. Jack Rachlin
U.S. Geological Survey
Geology, Rm 3 C136
Mail Stop 928 National Center
Reston, VA 22092

Art McGarr
U.S. Geological Survey, MS-977
345 Middlefield Road
Menlo Park, CA 94025

Dr. Robert Reinke
WL/NTESG
Kirtland AFB, NM 87117-6008

Richard Morrow
ACDA/VI, Room 5741
320 21st Street N.W
Washington, DC 20451

Dr. Byron Ristvet
HQ DNA, Nevada Operations Office
Attn: NVCG
P.O. Box 98539
Las Vegas, NV 89193

Dr. Keith K. Nakanishi
Lawrence Livermore National Laboratory
P.O. Box 808, L-205
Livermore, CA 94550

Dr. George Rothe
HQ AFTAC/TGR
Patrick AFB, FL 32925-6001

Dr. Carl Newton
Los Alamos National Laboratory
P.O. Box 1663
Mail Stop C335, Group ESS-3
Los Alamos, NM 87545

Dr. Michael Shore
Defense Nuclear Agency/SPSS
6801 Telegraph Road
Alexandria, VA 22310

Dr. Kenneth H. Olsen
Los Alamos Scientific Laboratory
P.O. Box 1663
Mail Stop C335, Group ESS-3
Los Alamos, NM 87545

Donald L. Springer
Lawrence Livermore National Laboratory
P.O. Box 808, L-205
Livermore, CA 94550

Howard J. Patton
Lawrence Livermore National Laboratory
P.O. Box 808, L-205
Livermore, CA 94550

Dr. Lawrence Turnbull
OSWR/NED
Central Intelligence Agency
Room 5G48
Washington, DC 20505

Mr. Chris Paine
Office of Senator Kennedy
SR 315
United States Senate
Washington, DC 20510

Dr. Thomas Weaver
Los Alamos National Laboratory
P.O. Box 1663, Mail Stop C335
Los Alamos, NM 87545

Colonel Jerry J. Perrizo
AFOSR/NP, Building 410
Bolling AFB
Washington, DC 20332-6448

J.J. Zucca
Lawrence Livermore National Laboratory
Box 808
Livermore, CA 94550

GL/SULL
Research Library
Hanscom AFB, MA 01731-5000 (2 copies)

Defense Intelligence Agency
Directorate for Scientific &
Technical Intelligence
Washington, DC 20301

Secretary of the Air Force (SAFRD)
Washington, DC 20330

AFTAC/CA
(STINFO)
Patrick AFB, FL 32925-6001

Office of the Secretary Defense
DDR & E
Washington, DC 20330

TACTEC
Battelle Memorial Institute
505 King Avenue
Columbus, OH 43201 (Final Report Only)

HQ DNA
Attn: Technical Library
Washington, DC 20305

DARPA/RMO/RETRIEVAL
1400 Wilson Boulevard
Arlington, VA 22209

DARPA/RMO/Security Office
1400 Wilson Boulevard
Arlington, VA 22209

Geophysics Laboratory
Attn: XO
Hanscom AFB, MA 01731-5000

Geophysics Laboratory
Attn: LW
Hanscom AFB, MA 01731-5000

DARPA/PM
1400 Wilson Boulevard
Arlington, VA 22209

Defense Technical Information Center
Cameron Station
Alexandria, VA 22314 (5 copies)